Journal of Medicinal Chemistry

pubs.acs.org/jmc Article

# Nature-Inspired (di)Azine-Bridged Bisindole Alkaloids with Potent Antibacterial *In Vitro* and *In Vivo* Efficacy against Methicillin-Resistant *Staphylococcus aureus*

Nidja Rehberg,[⊥] Gereon A. Sommer,[⊥] Daniel Drießen,[⊥] Marco Kruppa,[⊥] Emmanuel T. Adeniyi,[⊥] Shang Chen, Lin Wang, Karina Wolf, Boris O. A. Tasch, Thomas R. Ioerger, Kui Zhu, Thomas J. J. Müller,* and Rainer Kalscheuer*

Cite This: https://dx.doi.org/10.1021/acs.jmedchem.0c00826 Read Online

ACCESS | Metrics & More | Article Recommendations | Supporting Information

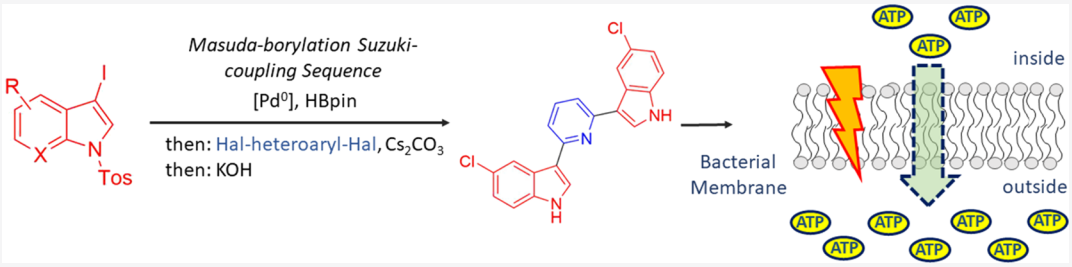


**ABSTRACT:** Natural bisindole alkaloids such as Hyrtinadine A and Alocasin A, which are known to exhibit diverse bioactivities, provide promising chemical scaffolds for drug development. By optimizing the Masuda borylation−Suzuki coupling sequence, a library of various natural product-derived and non-natural (di)azine-bridged bisindoles was created. While unsubstituted bisindoles were devoid of antibacterial activity, 5,5′-chloro derivatives were highly active against methicillin-resistant *Staphylococcus aureus* (MRSA) and further Gram-positive pathogens at minimal inhibitory concentrations ranging from 0.20 to 0.78 μM. These compounds showed strong bactericidal killing effects but only moderate cytotoxicity against human cell lines. Furthermore, the two front-runner compounds **4j** and **4n** exhibited potent *in vivo* efficacy against MRSA in a mouse wound infection model. Although structurally related bisindoles were reported to specifically target pyruvate kinase in MRSA, antibacterial activity of **4j** and **4n** is independent of pyruvate kinase. Rather, these compounds lead to bacterial membrane permeabilization and cellular efflux of low-molecular-weight molecules.

## HIGHLIGHTS

- The synthesis and characterization of bisindoles with heterocyclic bridges are reported.
- Synthetic nature-inspired bisindole derivatives were synthesized via a one-pot Masuda borylation−Suzuki coupling sequence.
- Bisindoles have promising *in vitro* and *in vivo* antibacterial activity against MRSA.
- Antibacterial activity of presented bisindoles is based on membrane permeabilization but not on inhibition of pyruvate kinase.

## INTRODUCTION

Since the introduction of penicillin, antibiotics have become one of the cornerstones of modern medicine. However, the number of multidrug-resistant bacterial pathogens steadily increased in the last years. Extensively drug-resistant strains, for which almost no antibiotic is clinically available anymore, became a major problem especially in hospitals and health care facilities and might reemerge as a major cause of morbidity and mortality even in industrialized regions of the world in the future unless effective countermeasures are rapidly implemented.[1] Hence, new lead structures addressing novel drug targets are urgently needed for many bacterial pathogens.[2] *Staphylococcus aureus* is a facultative pathogenic bacterium, which can cause wound infections, pneumonia, or sepsis.[3] β-Lactam antibiotics such as methicillin are the agents of choice for treatment of staphylococcus infections due to their good safety profiles. However, the widespread development of resistance against methicillin and other β-lactams as well as resistance to other antibacterial agents make treatment of *S. aureus* infections an increasing clinical challenge.[4]

Received: May 14, 2020







https://dx.doi.org/10.1021/acs.jmedchem.0c00826
J. Med. Chem. XXXX, XXX, XXX−XXX

**Scheme 1. Novel (di)Azine-Linked Bisindoles 4 via a Masuda−Suzuki Sequence**

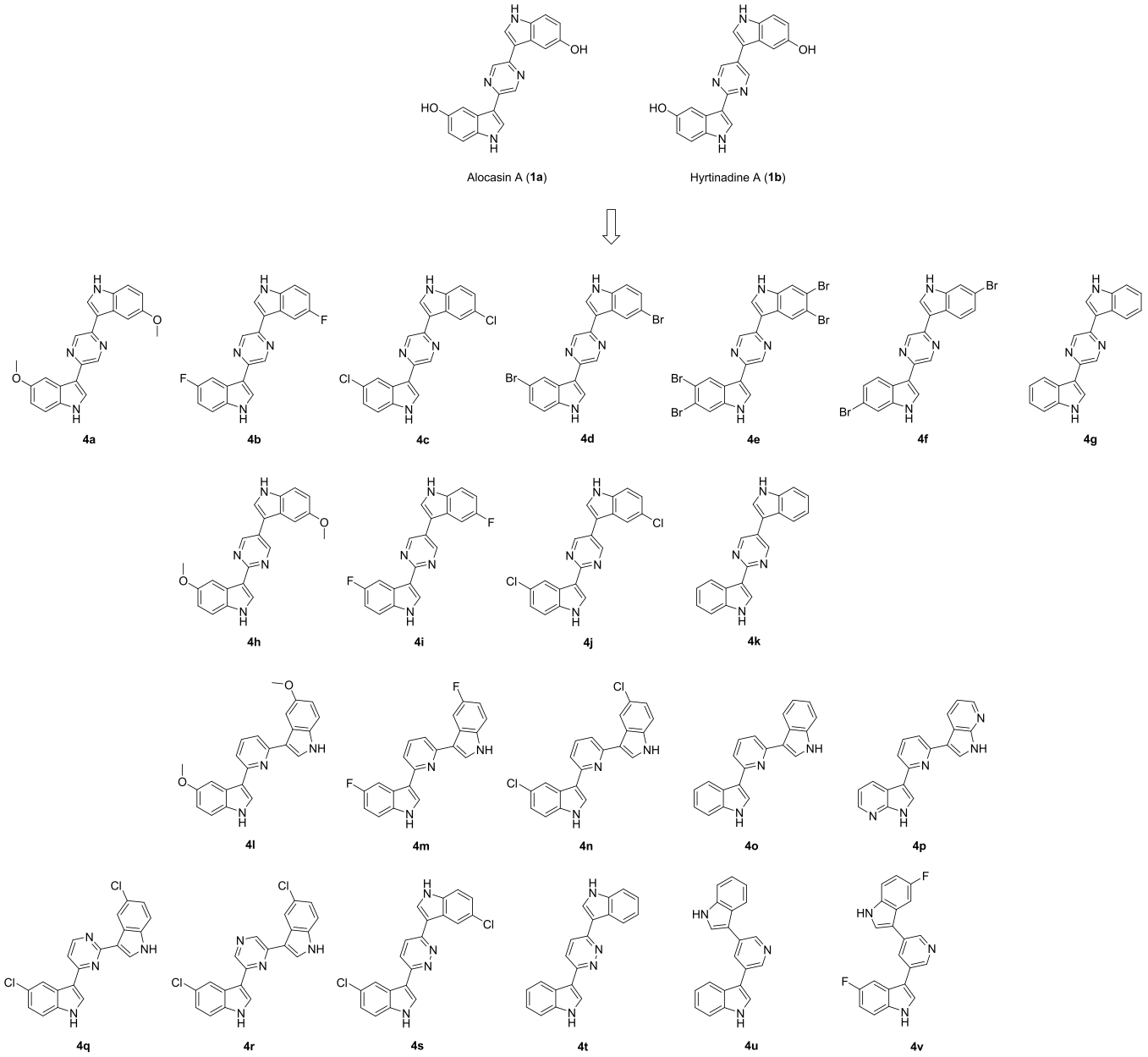


Approximately 70% of antibiotics are derived from natural compounds.[5] In addition to soil microbes and endophytes, also, plants and marine organisms like sponges can serve as sources for identifying new natural-sourced lead structures.[6] One promising class of antibacterial compounds is indole alkaloids, which have shown cytotoxic, antiviral, antimicrobial, antiparasitic, anti-inflammatory, and antifungal activity.[7−9] In particular, plant- and sponge-derived indole-containing alkaloids comprise metabolites with highly diverse bioactivities such as antitumor,[10,11] antifungal,[12] antiviral,[13] and also antimicrobial activity.[12,14] Two examples of natural bisindoles **1** are Alocasin A (**1a**) and Hyrtinadine A (**1b**), which consist of two indole moieties connected by a 2,5-substituted pyrazine or pyrimidine bridge. Alocasin A (**1a**) is produced by the Asian medicinal plant *Alocasia macrorrhiza* and possesses antifungal and cytostatic activity.[15] In contrast, Hyrtinadine A, produced from the Red Sea sponge *Hyrtios* sp., exhibited cytotoxicity against murine leukemia and human epidermoid carcinoma cells *in vitro*.[16] However, no antibacterial activity was reported for these natural core structures. Notwithstanding, the synthetic modification of natural compounds opens possibilities to find new antibacterial lead structures, creating new pharmacophores with higher antibacterial activity than the parental molecules.

The most commonly used method for the formation of carbon−carbon bonds between two $sp^2$ carbon atoms is the Suzuki−Miyaura coupling.[17] Starting from iodinated *N*-protected indoles **2** and suitable heterocyclic linkers **3**, the Suzuki coupling constitutes a highly reliable, versatile reaction, an ideal key step for the formation of (di)azine-linked bisindoles **4**. Furthermore, considerable functional group tolerance and applications of heteroaryls have been reported.[18,19] Since borylated starting materials are required, a preceding borylation of an electron-rich halogenated coupling partner in the presence of pinacolyl boran (HBpin) has to be performed. As a logical combination, the Pd-


https://dx.doi.org/10.1021/acs.jmedchem.0c00826
J. Med. Chem. XXXX, XXX, XXX−XXX

**Scheme 2. MBSC Pseudo Three-Component Synthesis of Bisindoles 4**

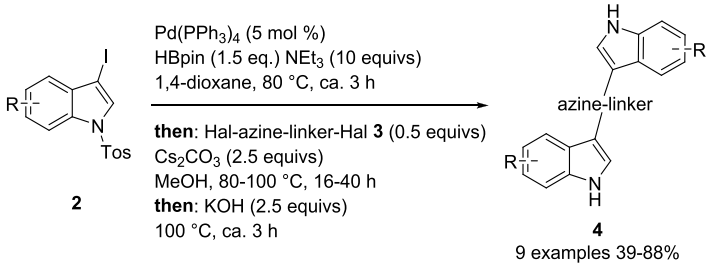


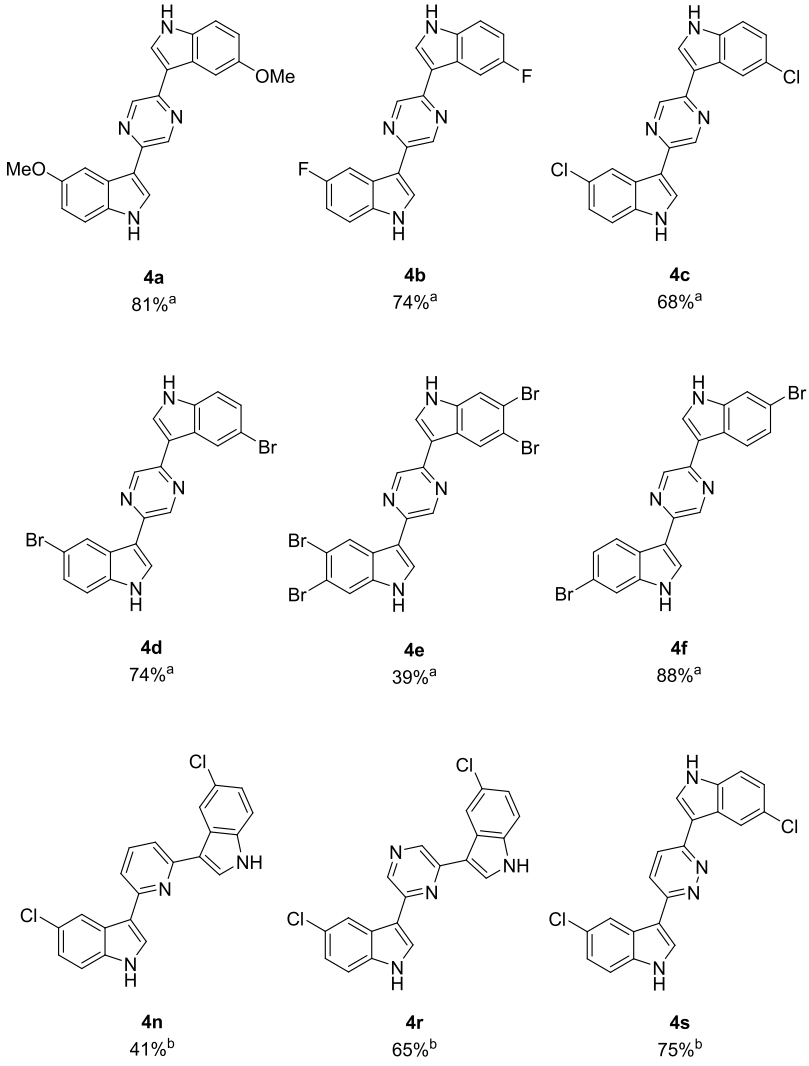


[a]10 mL of 1,4-dioxane and 7.0 mL of methanol. [b]4.0 mL of 1,4-dioxane and 3.0 mL of methanol.

catalyzed Masuda borylation[20] and the Suzuki arylation can be consecutively employed in the same reaction vessel.[19,21,22] For ligating two heteroaryl halides, this sequentially Pd-catalyzed one-pot reaction was developed and illustrated for the synthesis of marine alkaloids and derivatives.[19,23−25] Here, this one-pot methodology has now been employed for the synthesis of derivatives **4** of Hyrtinadine A and Alocasin A with different substitution patterns and also various central linkers **3** to establish structure−activity relationship studies with respect to antibacterial activity (Scheme 1). Moreover, optimized conditions for the synthesis of (di)azine-linked bisindoles **4** are reported.

## RESULTS AND DISCUSSION

**Synthesis of Bisindole Compounds 1 and 4.** Based on our previously established protocol, nine heteroaryl bridged bisindole molecules **4** were synthesized containing a pyridazine (**4s** and **4t**) or a pyridine bridge (**4l**−**4p**, **4u**, and **4v**) and eight with a pyrazine linker (**4a**−**4g** and **4r**). We recently showed the successful application of the Masuda borylation−Suzuki


https://dx.doi.org/10.1021/acs.jmedchem.0c00826
J. Med. Chem. XXXX, XXX, XXX−XXX

**Scheme 3. Synthesis of (di)Azine-Linked 3,3′-Bisindoles 4 via Optimized MBSC Sequences**

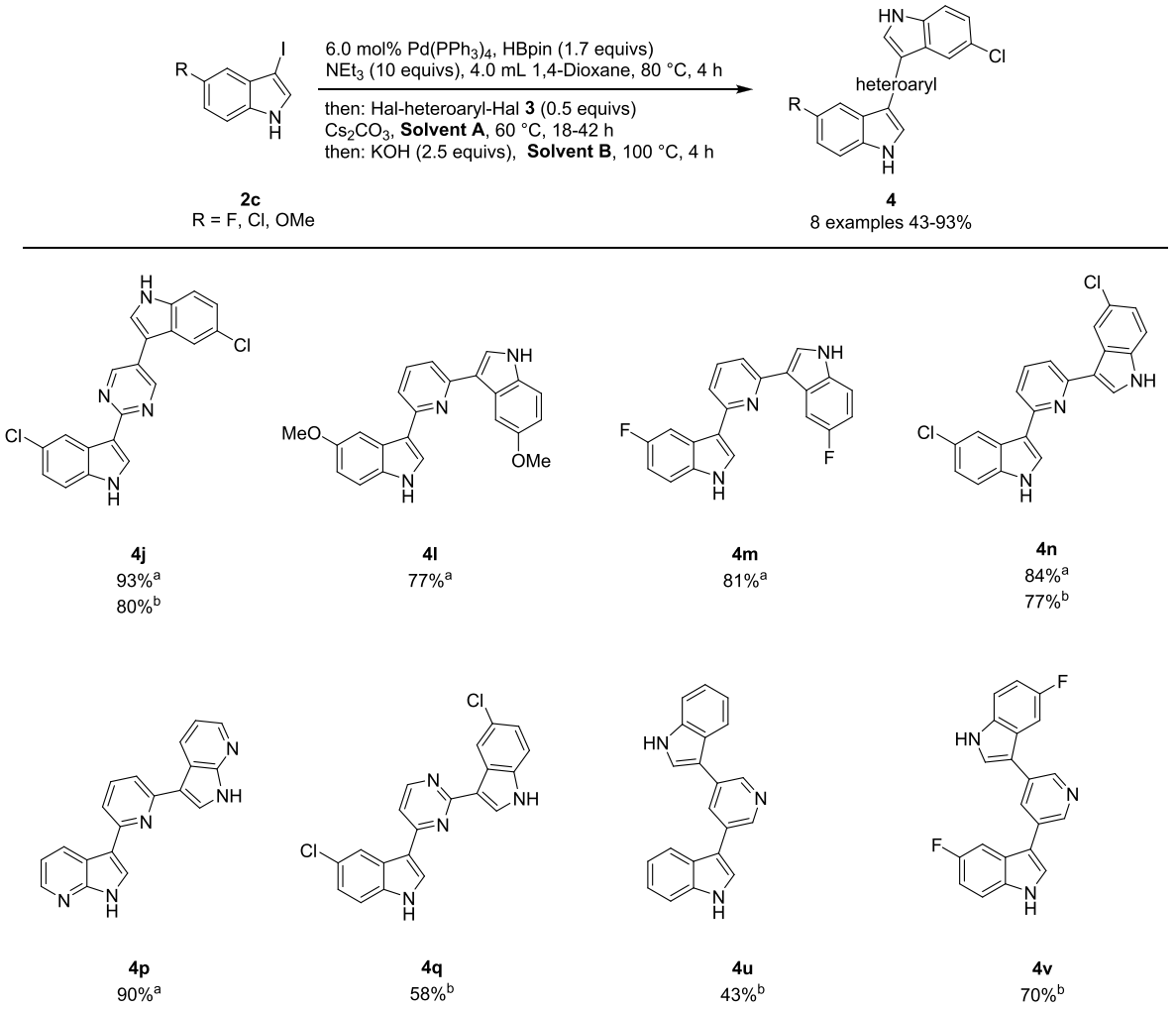


[a]Solvent A, 7.0 mL of MeOH; solvent B, /; $t_{SC}$, 18 h. [b]Solvent A, 3.0 mL of $H_2O$; solvent B, 4.0 mL of MeOH; $t_{SC}$, 42 h.

coupling (MBSC) as a one-pot reaction in the sense of a sequentially palladium-catalyzed pseudo three-component process.[25] In this study, Hyrtinadine A (**1b**) and several derivatives (**4h**−**4k**) were efficiently synthesized by this strategy, underlining the robustness of this synthetic tool for the concise preparation of bisindoles with different heterocyclic bridges (**4q**, **4s**, and **4t**) as well. A structurally related compound amenable to this synthetic protocol is the plant-derived alkaloid Alocasin A (**1a**).[15] Compounds **4a**−**4g** and **4r** can be considered Alocasin A analogues. We synthesized a small library of derivatives **4** of these natural products with different indole moieties. Recognizing the antibacterial potency especially of chlorinated compound **4c** in this portfolio, we established new chlorinated bisindole (**4n**, **4r**, and **4s**, Scheme 2) structures by variation of linker **3**.

The indoles **2** were prepared for the sequence according to Witulski et al.[26] The Masuda borylation of the indoles was performed in dry 1,4-dioxane with water-free triethylamine under an argon atmosphere at 80−100 °C (monitored by TLC). After full conversion of indole halide **2**, the excess of pinacolborane was quenched by addition of methanol. The resulting mixture was also desirable for the base cesium carbonate as methanol/carbonate mixtures are preferred for Suzuki coupling reactions. The cross-coupling was successfully performed at slightly higher temperatures. The commercially available dihaloazines **3** were employed without further purification. When using *N*-tosyl-indoles **2**, an additional cleavage step was necessary. Indeed, desulfonation is possible in a one-pot fashion by adding ground potassium hydroxide to the reaction mixture. Alocasin A (**1a**) was obtained from compound **4a** by demethylation in a mixture of aqueous hydrobromic acid (48%) and acetic acid at 120 °C. In comparison to previous studies on Masuda−Suzuki sequences,[23−25] the more reactive iodide Suzuki coupling partners **3** (increased rate of oxidative addition, the first step in a catalytic cross-coupling cycle) are more expensive and often less stable. However, it is noteworthy mentioning that there are far more commercially available bromides (and chlorides). Therefore, the scope of this one-pot process was probed with bromo and chloro derivatives of dihaloazines **3**. For minimizing side products and impurities, a short optimization study with 5-chloro-3-iodo-1-tosyl-1*H*-indole (**2a**) and 2,6-dibromopyridine (**3b**) in the model reaction was conducted (for details see the Supporting Information). Applying $H_2O$ as a cosolvent during Suzuki coupling finally gave high yields of the desired product, which was analytically pure after short column chromatography. Noteworthy, low temperatures, high concentration reaction mixtures, and longer reaction time gave the best


https://dx.doi.org/10.1021/acs.jmedchem.0c00826
J. Med. Chem. XXXX, XXX, XXX−XXX

**Table 1. Synthesized Substituted Compounds 1 and 4 and Their MIC against Methicillin-Resistant *S. aureus* Strain ATCC 700699 in $\mu$M and $\mu$g/mL[a]**

| | $MIC_{90}$ | | | $MIC_{90}$ | | | $MIC_{90}$ | |
|---|---|---|---|---|---|---|---|---|
| compound | $\mu$M | $\mu$g/mL | compound | $\mu$M | $\mu$g/mL | compound | $\mu$M | $\mu$g/mL |
| **1a** | >100 | >34.24 | **4f** | >100 | >46.82 | **4n** | 0.20 | 0.08 |
| **1b** | >100 | >34.24 | **4g** | >100 | >31.04 | **4o** | >100 | >30.94 |
| **4a** | >100 | >37.04 | **4h** | 50 | 18.52 | **4p** | >100 | >31.14 |
| **4b** | >100 | >34.63 | **4i** | 12.5 | 4.32 | **4q** | 3.13 | 1.19 |
| **4c** | 0.39 | 0.15 | **4j** | 0.39 | 0.15 | **4r** | 0.39 | 0.15 |
| **4d** | 1.56 | 0.73 | **4k** | 12.5 | 3.88 | **4s** | 0.78 | 0.30 |
| **4e** | 25 | 15.65 | **4l** | 12.5 | 4.62 | **4t** | >100 | >31.04 |

[a]The maximal tested concentration was 100 $\mu$M. $MIC_{90}$ > 100 $\mu$M is considered inactive.

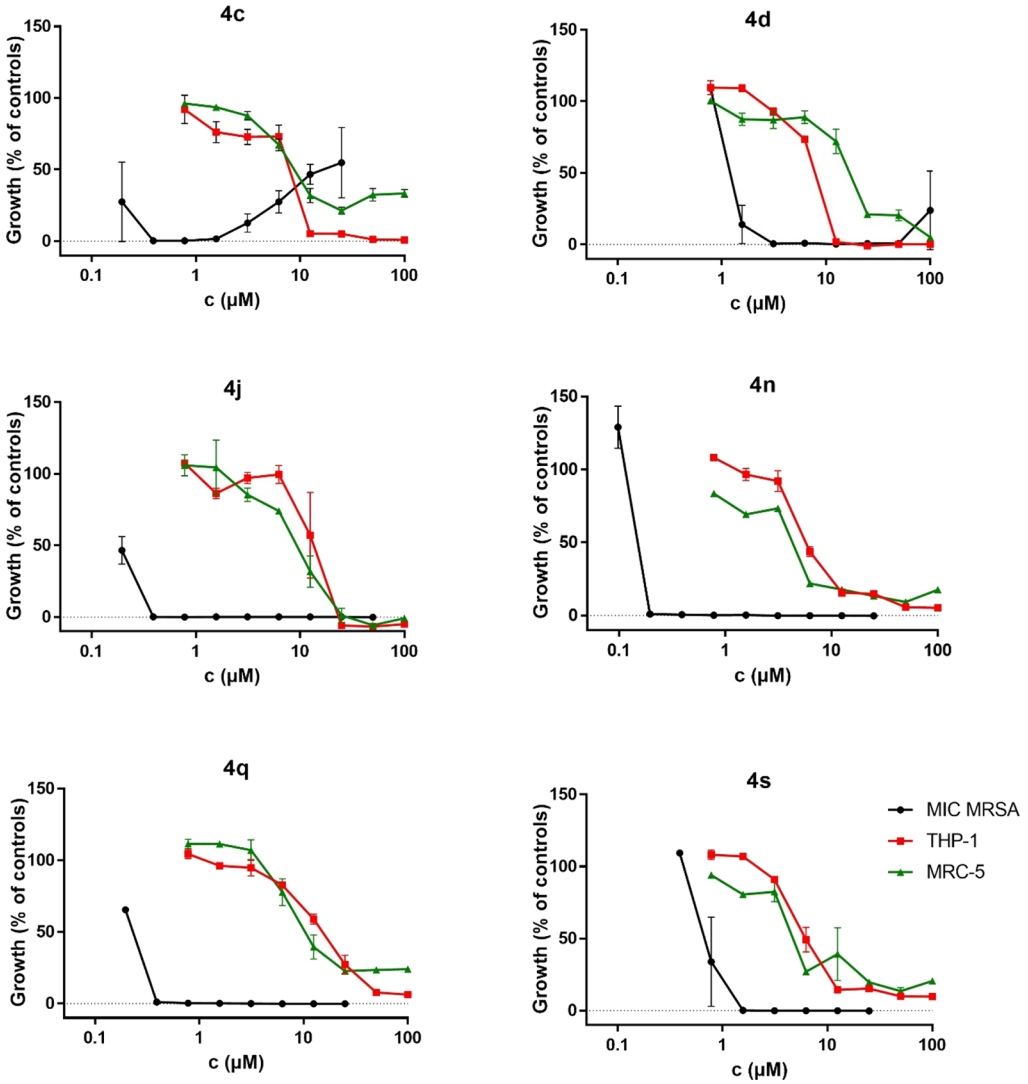


**Figure 1.** Dose–response curves of compounds **4c**, **4d**, **4j**, **4n**, **4q**, and **4s** against MRSA (circle) and human cell lines MRC-5 (triangle) and THP-1 (square). Data are means of triplicates ± SD. Growth was quantified using BacTiter-Glo assay for bacterial and resazurin dye reduction assay for eukaryotic growth. Resulting selectivity indices (SI = $IC_{50}/MIC_{90}$): **4d**, SI = 8; **4c**, SI = 32; **4j**, SI = 32; **4s**, SI = 8; **4q**, SI = 32; **4n**, SI = 32.

results. For further comparison, the best two conditions were used to synthesize different derivatives of 5,5′-chlorobisindoles **4** (Scheme 3).

While the initial conditions of the MBSC sequence were developed for a bi(hetero)aryl synthesis, an optimized process for creating an efficient pseudo three-component reaction employing bromides and chlorides now has been established. Most critically in the Suzuki coupling, water as a less nucleophilic cosolvent and lower reaction temperatures kinetically favor cross-coupling over competing nucleophilic aromatic substitution of the heteroaryl halides **3**, finally furnishing the desired bisindoles **4** in good yields. Therefore, the use of iodides is no longer necessary for obtaining pure compounds in a fast and convenient fashion. For isolating the


https://dx.doi.org/10.1021/acs.jmedchem.0c00826
J. Med. Chem. XXXX, XXX, XXX−XXX

Table 2. Checkerboard Analysis of Compound 4j and Colistin against Gram-Negative Bacteria[a]

| Gram-negative bacteria | MIC (μM) | | $FIC_a$ | $FIC_b$ | FICI | effect |
|---|---|---|---|---|---|---|
| | colistin | 4j | | | | |
| *K. pneumoniae* ATCC 700603 | 1.56 | >100 | ≤0.125 | 0.125 | ≤0.25 | synergistic |
| *P. aeruginosa* ATCC 27853 | 0.39 | >100 | ≤0.0625 | 1 | ≤1.0625 | additive |
| *A. baumannii* ATCC BAA-1605 | 0.78 | >100 | ≤0.0625 | 0.25 | ≤0.3125 | synergistic |
| *E. coli* ATCC BAA-2469 | 0.78 | >100 | ≤0.0313 | 0.064 | ≤0.0953 | synergistic |

[a]$FIC_a$ = MIC of the combination/$MIC_a$ alone; $FIC_b$ = MIC of the combination/$MIC_b$ alone; FICI = $FIC_a$ + $FIC_b$. a = **4j**; b = colistin. FICI was defined as follows: synergistic effect when FICI ≤ 0.5; partial synergistic effect when FICI > 0.5 ≤ 0.75; indifferent or additive effect when FICI > 0.75 ≤ 2; antagonistic effect when FICI > 2.

products directly from the reaction mixture, purification by fast and simple flash chromatography is sufficient. If methanol is used as a solvent for Suzuki coupling instead, further workup steps are required after chromatography.

In summary, by use of the Masuda borylation−Suzuki coupling (MBSC) sequence, a small but diverse library around the natural compounds Alocasin A and Hyrtinadine A was easily and efficiently synthesized now allowing detailed structure−activity relationship (SAR) studies regarding their antibacterial effects. Ten of these structures (**4b**, **4c**, **4e**, **4l**−**4n**, **4p**, **4q**, **4r**, and **4s**) were not described elsewhere before.

**Synthetic Bisindole Derivatives 1 and 4 Exhibit Potent Antibacterial Activity against a Panel of Pathogenic Bacterial Strains.** Minimal inhibitory concentrations (MICs) of all compounds **1** and **4** were determined by screening in two-fold serial dilution at a concentration range between 100 and 0.78 μM against Gram-positive nosocomial bacterial pathogens including methicillin-resistant *S. aureus* (MRSA), *Enterococcus faecalis*, and vancomycin-resistant *Enterococcus faecium*. None of the tested compounds **1** and **4** were active against the Gram-negative bacterium *Acinetobacter baumannii*, and they also showed no or only a weak effect against *Mycobacterium tuberculosis* (Supporting Information Table S1). However, compounds **1** and **4** showed variable inhibitory activity against the tested Gram-positive nosocomial strains. The observed antibacterial potencies highly depended on the substitution pattern at position 5′ and 5″ or 6′ and 6″ of the indole rings (Table 1). As already reported in the literature, the natural compounds Alocasin A (**1a**) and Hyrtinadine A (**1b**) were devoid of any inhibitory activity against the tested pathogenic bacteria. Also, 5′,5″-dimethoxylated (**4a** and **4h**) compounds did not show any (in the case of the pyrazine derivatives) or only a slight effect (in the case of the pyrimidine derivative) against *M. tuberculosis*, *S. aureus*, *E. faecalis*, and *E. faecium*. Interestingly, halogenation seemed to be essential for the antimicrobial activity. If the compound was halogenated at position 5′,5″ of the indole ring, the MICs against the MRSA strain decreased (**4b**−**4e**, **4i**, and **4j**). Regarding the halogenated derivatives **4b** and **4i** as well as **4c** and **4j**, it could also be observed that the replacement of fluorine by chlorine led to a decrease in the MIC by a factor ≥ 32. The replacement from chlorine to bromine increased the MIC slightly to 1.56 μM in the case of MRSA. Furthermore, the brominated structures **4d**−**4f** indicated that the halogenation at position 5′,5″ (**4d**) is critical regarding antibacterial activity. The additional halogenation at position 6′,6″ of the indole rings (**4e**) led to an increased MIC of 25−100 μM. If only position 6′,6″ was halogenated like in compound **4f**, no activity could be observed in the tested concentration range.

In contrast to these relatively narrow structural requirements regarding the indole moieties, wide flexibility was tolerated concerning the linker unit. Substitution of the linker from pyrimidine or pyrazine to pyridazine (**4s**) or the replacement of a 2,5-substitution to a 2,4-substituted pyrimidine ring (**4q**) or even the changing of the linker from pyrimidine to 3,5-disubstituted pyrazine (**4r**) or 2,6-disubstituted pyridine (**4n**) had only a slight influence on the MIC as long as the indole rings were substituted with a chlorine atom at the 5′,5″ position (Table 1).

Paradoxically, a decreased inhibitory effect for compounds **4c**, **4d**, and **4r** could be observed at concentrations higher than the MIC (Figure 1; Supporting Information Figure S1), whereas other symmetric compounds such as **4n** or **4s** did not show this effect. It is possible that **4c**, **4d**, and **4r** aggregate at higher concentrations because of their axial symmetry and precipitate, thus resulting in a decreased effective concentration of the compounds in solution. Since the other symmetrical compounds **4n** and **4s** did not show this effect, this has to be a peculiar influence of the pyrazine linker. However, solubility of all tested derivatives (**4c**, **4d**, **4j**, **4n**, and **4r**) was generally very low in aqueous buffer (Supporting Information Figure S2a, b, and e; Figure S3), so that the physicochemical basis of this differential effect of compounds **4c**, **4d**, and **4r** remains elusive.

Interestingly, the 5′,5″-chloro-pyrazine derivatives **4c** and **4r** exhibited a very narrow specificity by being exclusively active against the MRSA strain (MIC = 0.39−0.78 μM) but not the methicillin-sensitive parental *S. aureus* strain for yet unknown reasons. In contrast, brominated derivative **4e** showed an MIC of 1.56 μM against both *S. aureus* strains (Supporting Information Table S1). Only compounds **4j**, **4n**, and **4q** exhibited broad antibacterial potency against all tested Gram-positive nosocomial pathogens (Supporting Information Table S1), making them the most promising candidates for further characterization.

**Cytotoxicity and Therapeutic Index.** To analyze the therapeutic index of these structures, compounds **4c**, **4d**, **4j**, **4n**, **4q**, and **4s** were tested against the human THP-1 monocytic and MRC-5 lung fibroblast cell lines. Since the compounds were found to be cytotoxic only at concentrations ≥ 12.5 μM, the selectivity indices ($IC_{50}/MIC_{90}$) yielded sufficient therapeutic margins (Figure 1). **4j**, **4n**, and **4q** were additionally tested against human kidney HEK293, human hepatocellular carcinoma HepG2, and lung carcinoma CLS-54 cell lines. The three compounds were cytotoxic only at concentrations > 12.5 μM, confirming their rather low cytotoxic potential and resulting in sufficient antibacterial selectivity (Supporting Information Table S2). Furthermore, **4j** and **4n** exhibited no hemolytic activity against sheep erythrocytes even at high concentration up to 100 μM (Supporting Information Figure S4), further adding to their low general toxicity profile.


https://dx.doi.org/10.1021/acs.jmedchem.0c00826
J. Med. Chem. XXXX, XXX, XXX−XXX

**Table 3. Checkerboard Analysis of Compound 4n and Colistin against Gram-Negative Bacteria**[a]

| Gram-negative bacteria | MIC ($\mu$M) colistin | MIC ($\mu$M) **4n** | $FIC_a$ | $FIC_b$ | FICI | effect |
|---|---|---|---|---|---|---|
| *K. pneumoniae* ATCC 700603 | 1.56 | >100 | ≤0.125 | 0.125 | ≤0.25 | synergistic |
| *P. aeruginosa* ATCC 27853 | 0.39 | >100 | ≤0.0625 | 0.5 | ≤0.5625 | partially synergistic |
| *A. baumannii* ATCC BAA-1605 | 0.78 | >100 | ≤0.0625 | 0.25 | ≤0.3125 | synergistic |
| *E. coli* ATCC BAA-2469 | 0.78 | >100 | ≤0.0313 | 0.064 | ≤0.0953 | synergistic |

[a]$FIC_a$ = MIC of the combination/$MIC_a$ alone; $FIC_b$ = MIC of the combination/$MIC_b$ alone; FICI = $FIC_a$ + $FIC_b$. a = **4n**; b = colistin. FICI was defined as follows: synergistic effect when FICI ≤ 0.5; partial synergistic effect when FICI > 0.5 ≤ 0.75; indifferent or additive effect when FICI > 0.75 ≤ 2; antagonistic effect when FICI > 2.

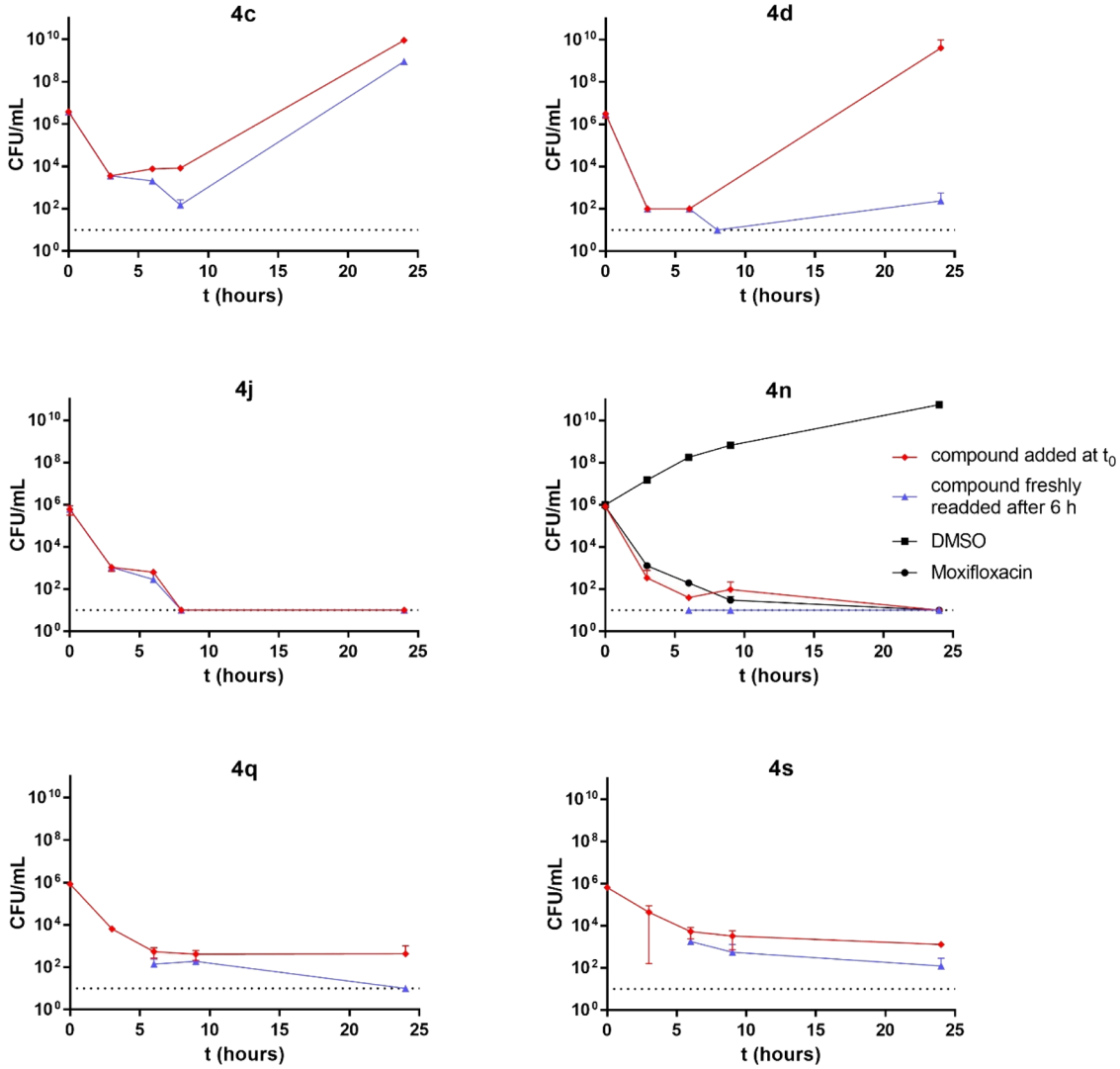


**Figure 2.** Time-kill curves of methicillin-resistant *S. aureus* (MRSA; ATCC 700699) for lead bisindoles **4c**, **4d**, **4j**, **4n**, **4q**, and **4s**. Compounds were tested at 5× MIC (resulting in 0.02−0.08% DMSO final concentration) (diamond). Additionally, in an independent experiment, the medium was replaced, and compounds were freshly readded after 6 h (triangle). Moxifloxacin at 5× MIC (circle) and cells grown in a medium without antibiotics but only containing 0.08% DMSO (square) were included as positive and negative controls, respectively. Results are presented as the mean of duplicate experiments ± SD.

**Outer Membrane Permeability Restricts Activity of Bisindole Alkaloids against Gram-Negative Bacteria.** The insusceptibility of Gram-negative bacteria to bisindoles prompted us to investigate whether the bacterial outer membrane restricts access of these compounds to their target(s). To assess this, we permeabilized the bacterial outer membrane with subinhibitory concentrations of colistin (COL)—an antibiotic whose mode of action entails disruption of the outer membrane in a lipopolysaccharide-dependent manner in Gram-negative bacteria.[27] All tested Gram-negative bacteria were initially insensitive to compounds **4j** and **4n**. However, upon permeabilization of the outer membrane with subinhibitory concentrations of COL, there was a moderate (in the case of *Pseudomonas aeruginosa*) to strong increase (in the case of all other tested strains) in susceptibility to both compounds. As indicated in Tables 2 and 3, the presence of


https://dx.doi.org/10.1021/acs.jmedchem.0c00826
J. Med. Chem. XXXX, XXX, XXX−XXX

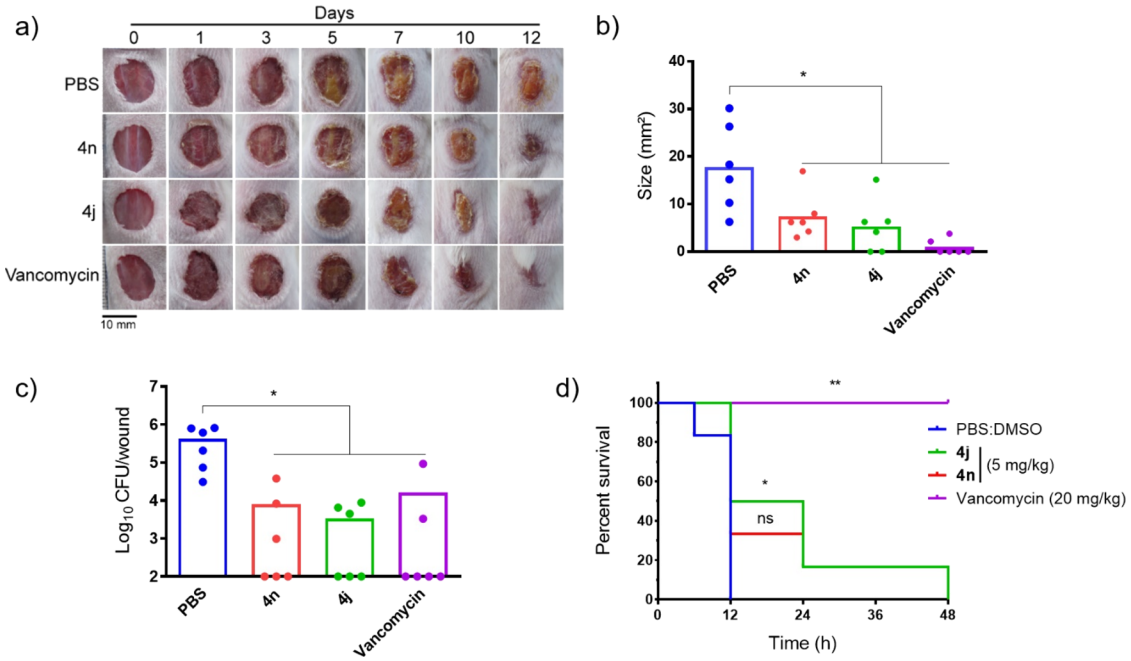


**Figure 3.** *In vivo* efficacy of bisindoles in mouse wound and peritonitis-sepsis infection models. (a) Pictures of skin wounds in a mouse skin wound infection model, treated with a single dose of **4j** or **4n** (each at 5 mg/kg). Vancomycin (20 mg/kg) and PBS were included as positive and negative controls, respectively. Bars represent 10 mm, $n = 6$. (b) Sizes of skin wounds and (c) bacterial counts in MRSA-infected wounds 12 days post-treatment with a single dose of **4j** or **4n** (each at 5 mg/kg). Vancomycin (20 mg/kg) and PBS were included as positive and negative controls, respectively. *P*-values were determined by the unpaired *t* test (*$p < 0.05$). $n = 6$. (d) Survival rates of mice in the mouse peritonitis-sepsis model. Six mice per group were infected via intraperitoneal injection with MRSA and treated one hour post-infection with single intraperitoneal doses of 5 mg/kg of **4j** or **4n**. Vancomycin (20 mg/kg) was used as a positive control. The percentage survival was calculated upon monitoring the mice for 48 h. *P*-values were determined by the logrank (Mantel−Cox) test (*$p < 0.05$; **$p < 0.01$; ns, not significant) and compared to PBS and vancomycin groups.

colistin at 0.064-fold MIC and 0.125-fold MIC robustly enhanced the susceptibility of *E. coli* (32-fold reduction in MIC) and *K. pneumoniae* (8-fold reduction in MIC) toward **4j** or **4n** resulting in FICI $\leq$ 0.0953 and $\leq$ 0.25, respectively, denoting a rather strong synergistic effect. On the other hand, the interaction between colistin and **4j** or **4n** yielded a partially synergistic and additive effect in the case of **4n** (FICI $\leq$ 0.5625) and **4j** (FICI $\leq$ 1.0625) against *P. aeruginosa*, respectively. Overall, this indicates that the intracellular target(s) of bisindoles is(are) present in Gram-negative bacteria but that the penetration of compounds into the cells is largely restricted by the outer membrane.

***In Vitro* Time-Kill Studies Revealed Early Bactericidal Activity.** Killing kinetics were measured to determine the potential bactericidal or bacteriostatic effect of the tested compounds on actively growing bacteria. For this, viable cell counts in treated samples were determined after different incubation times by employing colony forming unit (CFU) plating experiments. Compounds **4c**, **4d**, **4j**, **4n**, **4q**, and **4s** exhibited a strong bactericidal killing effect. After an incubation time of 6 h with compounds at five-fold MIC, bacterial viability was reduced by a factor of $10^4$−$10^5$ by substances **4d**, **4j**, **4n**, and **4q**, while treatment with compounds **4c** and **4s** reduced viability only 100-fold (Figure 2). Since after 24 h, the amount of surviving bacteria remained $<10^1$ CFU/mL (representing the limit of detection in this experiment) in the presence of compounds **4j**, **4n**, **4q**, and **4s**, these highly bactericidal substances might be able to completely sterilize the culture. In contrast, some persistent bacteria remained in the cultures containing **4c** and **4d** after 6 h of treatment, giving rise to an increasing number of cells again at prolonged treatment intervals. However, when these regrown cells were used to inoculate a fresh medium, the cultures still exhibited the same sensitivity like wild-type cells toward compounds **4c** and **4r**, indicating that they had not acquired genetically determined, inheritable resistance (data not shown). When compound **4c** was freshly added to cells after 6 h of incubation following washing and medium exchange, the viability of the culture continued to decrease to $10^2$ CFU/mL initially but almost rose to the same amount as the growth control after 24 h of incubation time (Figure 2), indicating that **4c** is either spontaneously or microbially degraded or metabolized to an inactive form under the tested assay conditions. Consequently, the stability of **4c** was evaluated over time. Since compound **4c** appears stable over a period of ca. 6 h (Supporting Information Figure S5) in aqueous solution, it is unlikely that compound **4c** substantially spontaneously degrades but rather is actively metabolized or modified by the bacteria, thereby resulting in reduction of the effective concentration of **4c**. Hence, its antibacterial effect wanes after 6 h of incubation. Interestingly, regrowth of the pathogen at extended incubation times was much less pronounced when compound **4d** was freshly added to the culture after 6 h (Figure 2). Therefore, substance **4d** might be less prone to degradation or depletion than structure **4c**.

**Bisindoles Exhibit Potent *In Vivo* Efficacy against MRSA in a Mouse Wound Infection Model.** Due to their potent bactericidal anti-MRSA *in vitro* activity, we evaluated the potential therapeutic effect of **4j** and **4n** in a mouse wound infection model. Skin wounds were infected with MRSA strain


https://dx.doi.org/10.1021/acs.jmedchem.0c00826
J. Med. Chem. XXXX, XXX, XXX−XXX

T144 (a multidrug-resistant clinical *S. aureus* isolate sensitive to vancomycin[28]) and subsequently treated one hour post-infection by **4j** or **4n** (each at 5 mg/kg) employing a single-dose topical application. Treatment with both compounds promoted skin wound healing when compared to those treated with PBS (negative control) (Figure 3a and b). The effect was comparable to that of vancomycin treatment at 20 mg/kg (positive control). Likewise, both compounds significantly reduced the bacterial burden in treated wounds comparable to vancomycin treatment at a 4-fold lower dose (5 mg/kg vs. 20 mg/kg) (Figure 3c).

Next, the systemic therapeutic effect of **4j** and **4n** was evaluated in a mouse peritonitis-sepsis model. Both compounds somewhat prolonged survival of infected mice, but the effect was weaker compared to vancomycin treatment (Figure 3d). Although the survival effect was statistically significant for **4j** and both compounds could only be tested at a 4-fold lower dose compared to vancomycin (5 mg/kg vs. 20 mg/kg body weight) due to limited compound availability, the overall systemic activity of both compounds seems to be limited, presumably as a result of their poor aqueous solubility (Supporting Information Figure S2c and d). This limitation needs to be addressed in future optimization of the compounds.

**Antibacterial Efficacy of Bisindole Derivatives 4 Is Independent of Pyruvate Kinase.** Several marine and synthetic bisindoles have been shown to inhibit enzymatic activity of pyruvate kinase (PK) of MRSA *in vitro*.[29−32] PK catalyzes the final reaction step in glycolysis generating pyruvate by transfer of a phosphoryl group from phosphoenolpyruvate to ADP. PK has been reported to be essential for *S. aureus* with inhibition leading to an impaired metabolism by reduced ATP production.[33] The essentiality of PK makes the enzyme a promising potential new drug target. Due to their structural similarity, it was reasonably conceivable that bisindole derivatives **4** also inhibit PK. This assumption was further supported by the fact that published bisindoles followed a similar SAR trend with halogenated derivatives inhibiting growth stronger than hydroxyl substitution at the indole rings.[29]

To assess involvement of PK as a potential molecular target of bisindole derivatives **4** in *S. aureus*, we determined the MIC of **4c**, **4d**, **4j**, **4n**, **4q**, and **4s** against the MRSA LAC wild-type strain and against the isogenic PK knock-out strain in a minimal medium with glucose or pyruvate as a single carbon source. The PK encoding gene *pyk* is conditionally essential in *S. aureus*. A *pyk* deletion mutant is viable in a medium that lacks glucose when it is supplemented with pyruvate. Indeed, the LAC Δ*pyk*::Erm$^R$ mutant was unable to grow in a medium containing glucose as a carbon source consistent with a previous report,[34] demonstrating PK essentiality under these conditions. Consistently, the MRSA LAC wild-type was fully susceptible to compound **4j** during growth on glucose (Figure 4). However, unexpectedly, this strain showed unaltered susceptibility to **4j** in a medium containing pyruvate as the sole carbon source, a condition where PK activity is dispensable. Furthermore, the isogenic PK-deficient LAC Δ*pyk*::Erm$^R$ mutant was even slightly more sensitive toward **4j** during growth on pyruvate, while it was expected to be resistant if the compound specifically targets PK in the bacterial cell (Figure 4). Similar susceptibility patterns were also observed for compounds **4d**, **4n**, **4q**, and **4s** (Supporting Information Figure S6).

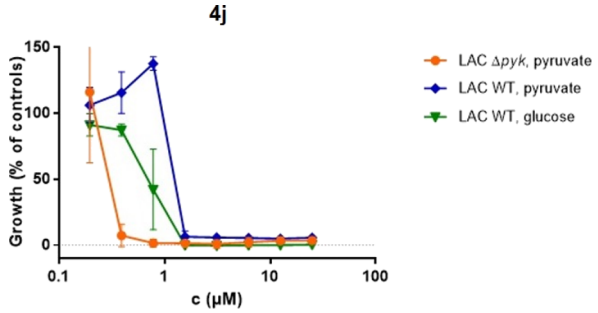


**Figure 4.** Antibacterial activity of **4j** against cells of MRSA LAC wild-type and LAC Δ*pyk*::Erm$^R$ in a minimal M9 medium with glucose (triangle) or pyruvate (circle, diamond) as a sole carbon source. Data are means of duplicates ± SD. Growth was quantified using the resazurin reduction assay.

To directly evaluate the involvement of PK as a potential molecular target of bisindole alkaloids **4**, an N-terminally His6-tagged version of *S. aureus* PK was heterologously expressed in *E. coli* NiCo21(DE3) and purified employing nickel-NTA affinity chromatography (Figure 5a). The enzymatic activity of purified recombinant *S. aureus* PK, however, was not inhibited by compounds **4j**, **4n**, and **4q** up to concentrations of 12.5 μM (Figure 5b), which is well above the MICs for these compounds against whole cells of *S. aureus* (Table 1). Additionally, also commercially available rabbit muscle PK, which is 97% identical to isoform M1 of human PK and 45% identical to MRSA PK, was completely insensitive to the tested compounds (Figure 5b), indicating a general lack of inhibitory properties toward PK enzymes.

In combination, these findings clearly demonstrate that the bactericidal activity of bisindole derivatives **4** on *S. aureus* cells is entirely *pyk*-independent under the tested *in vitro* culture conditions.

**Resistance Studies.** In order to reveal insights into the *pyk*-independent mechanism of antibacterial activity of the reported bisindole derivatives, we attempted to isolate spontaneous mutants of *S. aureus* MRSA strain ATCC 700699 resistant to **4j** on a solid medium. However, generation of single-step resistant mutants on agar supplemented with varying concentrations of bisindoles was unsuccessful. Thus, cells of *S. aureus* MRSA strain ATCC 700699 were serially passaged in a liquid medium with escalating subinhibitory concentrations of **4j**. After 38 culture passages, **4j**-resistant MRSA mutants exhibiting low-level resistance (2- to 4-fold shift in MIC) were obtained. As expected, whole genome sequencing revealed that the mutants had accumulated several mutations (Supporting Information Table S3). However, none of them pointed toward an obvious specific gene product that could be mediating resistance or directly representing a potential target. Furthermore, cross-resistance was observed among bisindoles since **4j**-resistant MRSA mutants were also resistant to **4n** with a similar 2-fold shift in MIC. In contrast, no cross-resistance was observed for antibiotics of other classes such as vancomycin, moxifloxacin, linezolid, and ramoplanin (Supporting Information Table S4), suggesting that the mechanism of resistance toward bisindoles in the studied MRSA mutants, while still elusive, is bisindole-specific.

**Mode of Action Studies.** One of the hallmarks of membrane-targeting antimicrobials is reduced potential for the emergence of bacterial resistance.[35] In like manner, difficulty in resistance generation and low-level resistance in


https://dx.doi.org/10.1021/acs.jmedchem.0c00826
J. Med. Chem. XXXX, XXX, XXX−XXX

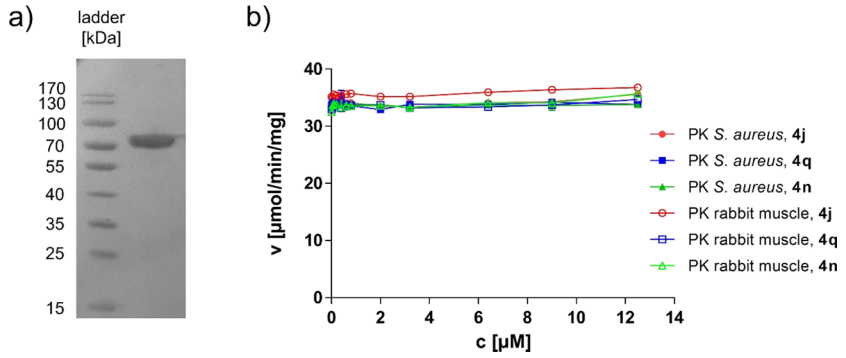


**Figure 5.** Bisindole derivatives **4j**, **4n**, and **4q** not inhibiting pyruvate kinase (PK) enzymatic activity *in vitro*. (a) Coomassie stained SDS-PAGE of N-terminally His6-tagged *S. aureus* PK heterologously expressed in *E. coli* NiCo21 (DE3) and purified using Ni-NTA affinity chromatography. The sample was concentrated and desalted. Purified recombinant PK (1 $\mu$g) was applied to the gel. (b) Activity of PK from *S. aureus* (filled symbols) and from rabbit muscle (empty symbols) in the presence of **4j** (red circles), **4n** (green triangles), and **4q** (blue squares). Initial enzyme velocity ($v$), expressed as $\mu$mol/min/mg protein, is plotted against 12 different compound concentrations ranging from 0 to 12.5 $\mu$M. Data are means of triplicates ± SEM, measured in two independent experiments.

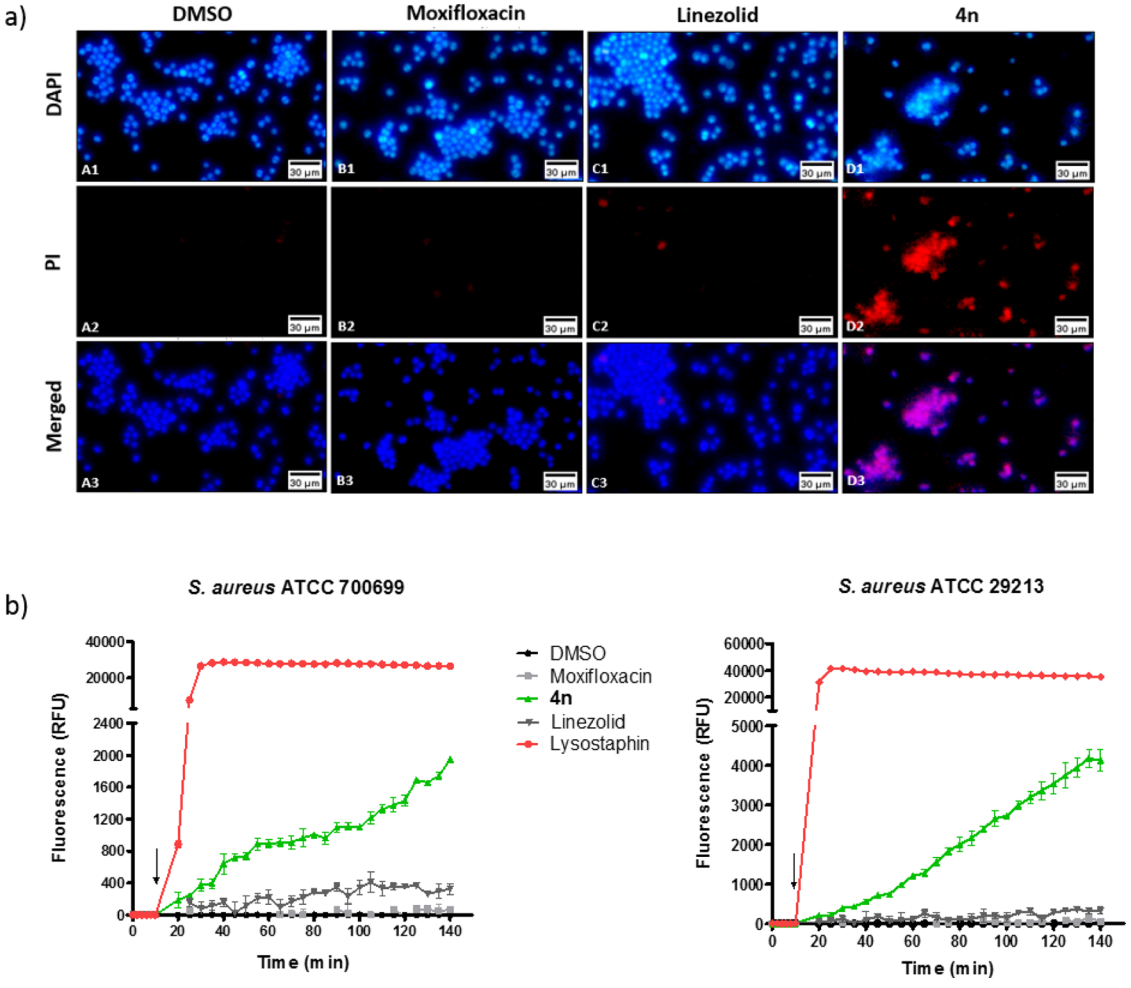


**Figure 6.** Membrane permeabilization of *S. aureus* cells by compound **4n**. (a) Fluorescence micrographs of *S. aureus* ATCC 29213 cells treated with 5-fold MIC of **4n** for 30 min. DMSO, moxifloxacin, and linezolid treatment served as negative controls. DAPI stains all cells irrespective of membrane integrity, whereas PI only stains cells with a permeabilized membrane. Bars represent 30 $\mu$m. (b) Propidium iodide internalization by **4n**-treated methicillin-resistant and susceptible *S. aureus* cells. PI fluorescence (excitation, 535 nm; emission, 617 nm) of cells incubated with 5-fold MIC of **4n** (green) in a black 96 well plate was measured for 2 h. Baseline fluorescence of untreated cells was established for 10 min before addition of compounds (black arrow). DMSO (0.078%), moxifloxacin, and linezolid were included as negative controls, while 10 $\mu$g/mL lysostaphin served as a positive control. Data are means of triplicates ± SEM.

conjunction with rapid bactericidal activity exhibited by bisindoles are somewhat indicators that the target of bisindoles might not be a protein but rather the bacterial membrane or cell wall. Thus, the possibility of bisindoles interacting with the


https://dx.doi.org/10.1021/acs.jmedchem.0c00826
J. Med. Chem. XXXX, XXX, XXX−XXX

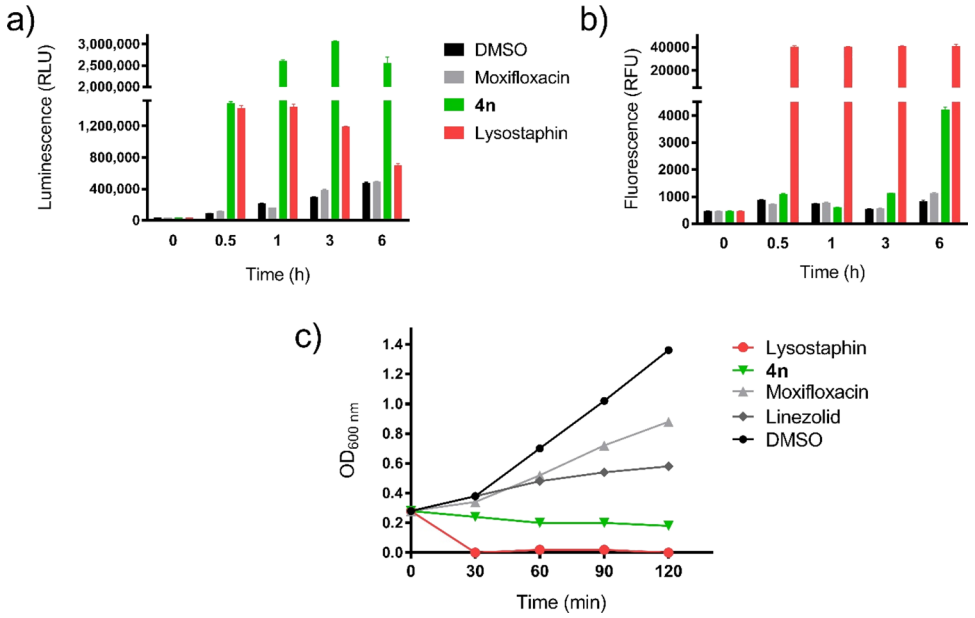


**Figure 7.** Leakage of intracellular contents and assessment of potential cell lysis of compound-treated *S. aureus* ATCC 700699. Efflux of (a) ATP and (b) GFP from **4n**-treated recombinant *S. aureus* ATCC 700699 cells expressing GFP. Cultures were treated with 5-fold MIC of **4n**. Release of ATP into cell-free culture supernatants was quantified using the bioluminescence-based BacTiter-Glo kit. The GFP level in cell-free culture supernatants at varying time points was quantified via GFP fluorescence at excitation and emission wavelengths of 475 and 509 nm, respectively. For both assays, moxifloxacin at 5-fold MIC and 0.078% DMSO served as negative controls, while 10 $\mu$g/mL lysostaphin was used as a positive control. Data are means of triplicates ± SEM. (c) Assessment of potential lysis of *S. aureus* ATCC 700699 cells induced by treatment with **4n**. Cells were incubated with 8-fold MIC of compounds. Optical density of cultures was measured at 600 nm. Decrease in turbidity would indicate lysis. Moxifloxacin and linezolid served as negative controls, 10 $\mu$g/mL lysostaphin served as a positive control, and 0.125% DMSO was used as a solvent and growth control.

bacterial membrane and/or cell wall was investigated by fluorescence microscopy using a double staining approach. Cells of MSSA strain ATCC 29213 were treated with **4n** and then costained with propidium iodide (PI) and 4′,6-diamidino-2-phenylindole (DAPI). DAPI, as a membrane permeant dye, can stain the minor groove of double-stranded DNA of cells regardless of their viability or membrane integrity. However, PI only enters the cell and subsequently intercalates DNA upon loss of membrane integrity.[36] MSSA cells incubated with a solvent control as well as non-membrane-targeting antibiotics such as moxifloxacin and linezolid exhibited negligible PI staining. On the other hand, cells treated with **4n** showed remarkable PI staining as soon as after 30 min incubation (Figure 6a), indicating substantial membrane permeabilization. Membrane permeability by **4n** was further evaluated via PI internalization assay. The effects of moxifloxacin, linezolid, lysostaphin, and **4n** on cells of MRSA strain ATCC 700699 and MSSA strain ATCC 29213 incubated with PI are depicted in Figure 6b. Lysostaphin, a bacteriolytic enzyme capable of punching holes in the cell wall of *Staphylococcus* species thereby causing rapid cell lysis,[37] was used as a positive control. As expected, lysostaphin showed a robust ability to permeabilize the bacterial membrane. In like manner, compound **4n** also instigated a gradual, yet conspicuous increase in fluorescence intensity, pointing to the fact that compound **4n** causes pronounced membrane permeabilization. In contrast, cells incubated with negative controls (linezolid and moxifloxacin, antibiotics impeding bacterial growth by inhibiting DNA gyrase and initiation of protein synthesis, respectively) induced very minor to no fluorescence as expected. This result is consistent with the fluorescence microscopy observations.

To corroborate the membrane-targeting features of bisindoles, cellular ATP and GFP leakage assays were conducted using the GFP-expressing recombinant *S. aureus* ATCC 700699 strain. In contrast to moxifloxacin and linezolid, **4n** as well as lysostaphin induced substantial leakage of ATP from the cells as early as 0.5 h of treatment (Figure 7a), while no leakage of ATP occurs from intact cells.[38] In contrast, release of GFP was only evident after 6 h incubation for **4n**-treated cells, whereas lysostaphin treatment resulted in rapid GFP efflux (Figure 7b). Next, we performed an experiment assessing potential bacterial cell lysis. **4n** did not induce substantial cell lysis since there was only a very slow and minor decrease in the optical density of the bacterial liquid culture over time in contrast to lysostaphin, which caused a rapid and strong decrease in the optical density (Figure 7c). Membrane-targeting agents generally give rise to initial rapid loss of low-molecular-weight compounds such as ATP (molecular weight 0.5 kDa) from within the cell due to a membrane injury.[39] Considering that GFP is a macromolecule with a molecular weight of 26.9 kDa, the presented results suggest that the reported bisindoles give rise to small pores in membranes of bacteria causing efflux of low-molecular-weight molecules, which provokes rapid cell death. Only after prolonged incubation times, the membrane is likely further permeabilized to also allow efflux of macromolecules, whereas the cell wall integrity is largely maintained so that no substantial cell lysis occurs.

## CONCLUSIONS

In summary, here, we report on the efficient synthesis of new derivatives **4** of the natural compounds Alocasin A (**1a**) and Hyrtinadine A (**1b**) and their strong antibacterial effect


https://dx.doi.org/10.1021/acs.jmedchem.0c00826
J. Med. Chem. XXXX, XXX, XXX−XXX

**Table 4. Experimental Details of the One-Pot Masuda–Suzuki Synthesis of the Alocasin A and Hyrtinadine A Derivatives 4a–4f, 4n, and 4r–4s**

| entry | 3-iodo indole **2** [mg] ([mmol]) | $t_1$ [h] | heteroaryl dihalide **3** [mg] ([mmol]) | $t_2$ [h] [(T)] | yield [mg] (%) |
|---|---|---|---|---|---|
| 1[a] | 427 (1.00) of 3-iodo-5-methoxy-1-tosyl-1*H*-indole (**2a**) | 3 | 119 (0.5) of 2,5-dibromopyrazine (**3a**) | 16 (100) | 150 (81) of **4a** |
| 2[a] | 415 (1.00) of 3-iodo-5-fluoro-1-tosyl-1*H*-indole (**2b**) | 3 | 118 (0.5) of 2,5-dibromopyrazine (**3a**) | 16 (100) | 128 (74) of **4b** |
| 3[a] | 432 (1.00) of 5-chloro-3-iodo-1-tosyl-1*H*-indole (**2c**) | 3 | 119 (0.5) of 2,5-dibromopyrazine (**3a**) | 16 (100) | 130 (68) of **4c** |
| 4[a] | 476 (1.00) of 3-iodo-5-bromo-1-tosyl-1*H*-indole (**2d**) | 3 | 119 (0.5) of 2,5-dibromopyrazine (**3a**) | 16 (100) | 172 (74) of **4d** |
| 5[a] | 501 (1.00) of *tert*-butyl-5,6-dibromo-3-iodo -1*H*-indole-1-carboxylate (**2e**) | 3 | 119 (0.5) of 2,5-dibromopyrazine (**3a**) | 16 (100) | 122 (39) of **4e** |
| 6[a] | 476 (1.00) of 3-iodo-6-bromo-1-tosyl-1*H*-indole (**2f**) | 3 | 119 (0.5) of 2,5-dibromopyrazine (**3a**) | 16 (100) | 206 (88) of **4f** |
| 7[b] | 432 (1.00) of 5-chloro-3-iodo-1-tosyl-1*H*-indole (**2c**) | 3 | 119 (0.5) of 2,6-dibromopyridine (**3b**) | 16 (80) | 77 (41) of **4n** |
| 8[b] | 432 (1.00) of 5-chloro-3-iodo-1-tosyl-1*H*-indole (**2c**) | 3 | 119 (0.5) of 2,6-dibromopyrazine (**3c**) | 40 (80) | 124 (65) of **4r** |
| 9[b] | 432 (1.00) of 5-chloro-3-iodo-1-tosyl-1*H*-indole (**2c**) | 3 | 166 (0.5) of 3,6-dibromopyridazine (**3d**) | 40 (80) | 0.143 (75) of **4s** |

[a]10 mL of 1,4-dioxane and 7.0 mL of methanol. [b]4.0 mL of 1,4-dioxane and 3.0 mL of methanol.

especially against MRSA. With respect to further preclinical development, compounds **4j** and **4n** seem to be most promising due to their broad antibacterial potency against all tested Gram-positive nosocomial pathogens, their moderate cytotoxicity toward human cells, and their *in vivo* efficacy in a mouse wound infection model upon topical application. Consequently, these compounds are interesting lead structures for further preclinical development with acceptable therapeutic margins. Future medicinal chemical optimization should focus on increasing their aqueous solubility to improve the systemic potency of the compounds. Despite structural similarity to bisindoles that were reported to inhibit PK of *S. aureus*, PK plays no role in explaining the strong bactericidal potency of compounds **4**. In contrast, we demonstrated that the reported molecules **4** likely target the bacterial membrane leading to permeabilization that causes rapid efflux of low-molecular-weight intracellular metabolites. Further studies are necessary to decipher the exact molecular target(s) and mode of interaction with the membrane of these potent bactericidal substances.

## EXPERIMENTAL SECTION

**Chemistry.** The synthesis of compounds **1b**, **4g–4i**, **4k**, **4o**, and **4t** has previously been published.[25] Compounds **1a**, **4a–4f**, **4n**, and **4r–4s** were synthesized and isolated as described below. Compounds **4j**, **4l–4n**, **4p–4q**, **4u**, and **4v** were synthesized and isolated under optimized conditions. Purity of all compounds is >95% as determined by combustion analysis. In some cases, purity was determined by HPLC and is stated in the analytical data of the compound.

**General Procedure.** 3-Iodo indole **2** (1.00 mmol) and tetrakis-(triphenylphosphane)palladium(0) were dissolved in dry 1,4-dioxane in a dry Schlenk tube with a magnetic stir bar under dry nitrogen (for experimental details, see Table 4). Triethylamine and 4,4,5,5-tetramethyl-1,3,2-dioxaborolane were added dropwise, and the reaction mixture was stirred at 80 °C for the times ($t_1$) indicated. Thereafter, the mixture was cooled to room temperature, and methanol, cesium carbonate (0.82 g, 2.50 mmol), and heteroaryl dihalide **3** (0.5 mmol) were added to the reaction mixture. This mixture was stirred at 80–100 °C for the times ($t_2$) indicated. Subsequently, the mixture was cooled to room temp., potassium hydroxide (0.14 g, 2.5 mmol) was added, and the reaction was stirred again at 100 °C for 2.5 h. After cooling to room temp., the mixture was diluted with dichloromethane, adsorbed on Celite under reduced pressure, and purified by column chromatography on silica gel (100:1:1 dichloromethane/MeOH/aq. $NH_3$ 25%). The resulting solid was then dried for 16 h under reduced pressure ($3 \times 10^{-3}$ mbar). Finally, the compounds **4** were suspended in dichloromethane and subsequently in *n*-hexane for further purification.

**Demethylation of Compound 3a to Give Alocasin A (1a).** Compound **4a** (226 mg, 0.61 mmol) is suspended in acetic acid (5 mL) and hydrobromic acid (5 mL, 48% aq.) and heated for 16 h to 120 °C in a closed Schlenk tube with a magnetic stir bar. After cooling to room temp., the solvents were removed under reduced pressure; the residue was suspended in ca. 25% aqueous $NH_3$ (25 mL) and stirred at room temp. for 1 h. The mixture was extracted with ethyl acetate (2 × 25 mL), and the organic layers are separated and dried (anhydrous sodium sulfate). The product was adsorbed on Celite and purified by column chromatography on silica gel (100:1:1 DCM/MeOH/25% aq. $NH_3$). The resulting solid was then dried under reduced pressure ($3 \times 10^{-3}$ mbar) for 16 h.

Alocasin A (**1a**) (150 mg, 72%); Mp, >300 °C. $^1$H NMR (600 MHz, DMSO-$d_6$): $\delta$ 6.70 (dd, $J$ = 8.6, 2.4 Hz, 2H), 7.26 (d, $J$ = 8.6 Hz, 2H), 7.81 (d, $J$ = 2.4 Hz, 2H), 8.11 (d, $J$ = 2.8 Hz, 2H), 8.82 (s, 2H), 9.00 (s, 2H), 11.34 (d, $J$ = 2.8 Hz, 2H) (see Supporting Information Figure S7). $^{13}$C NMR (151 MHz, DMSO-$d_6$) $\delta$ 105.5, 111.9, 112.1, 112.1, 125.6, 125.9, 131.3, 139.6, 146.5, 151.6 (see Supporting Information Figure S8). HR-MS (ESI) $m/z$: calcd for $[C_{20}H_{14}N_4O_2 + H]^+$, 343.1190; found, 343.1194. HPLC, 98.04%.

2,5-Bis(5-methoxy-*1H*-indole-3-yl)pyrazine (**4a**) (150 mg, 81%); Mp, 263 °C. $^1$H NMR (300 MHz, DMSO-$d_6$) $\delta$ 3.83 (s, 6H), 6.85 (dd, $J$ = 8.8, 2.5 Hz, 2H), 7.37 (dd, $J$ = 8.8, 0.6 Hz, 2H), 7.97 (d, $J$ = 2.5 Hz, 2H), 8.20 (d, $J$ = 2.8 Hz, 2H), 9.13 (s, 2H), 11.49 (d, $J$ = 2.9 Hz, 2H) (see Supporting Information Figure S9). $^{13}$C NMR (75 MHz, DMSO-$d_6$) $\delta$ 55.3, 103.1, 111.9, 112.4, 112.4, 125.6, 125.9, 131.9, 139.8, 146.5, 154.1 (see Supporting Information Figure S10). HR-MS (ESI) $m/z$: calcd for $(C_{22}H_{18}N_4O_2 + H)^+$, 371.1503; found, 371.1504. Anal calcd for $C_{22}H_{18}N_4O_2$ (370.4): C, 71.34; H, 4.90; N, 15.13; found: C, 71.20; H, 4.93; N, 15.13.

2,5-Bis(5-fluoro-*1H*-indole-3-yl)pyrazine (**4b**) (128 mg, 74%); Mp, 280 °C. $^1$H NMR (300 MHz, DMSO-$d_6$) $\delta$ 7.06 (ddd, $J$ = 9.1, 9.1, 2.7 Hz, 2H), 7.49 (dd, $J$ = 8.9, 4.6 Hz, 2H), 8.18 (dd, $J$ = 10.6, 2.6 Hz, 2H), 8.34 (d, $J$ = 2.8 Hz, 2H), 9.15 (s, 2H), 11.76 (d, $J$ = 1.9 Hz, 2H) (see Supporting Information Figure S11). $^{13}$C NMR (75 MHz, DMSO-$d_6$) $\delta$ 106.1 (d, $J$ = 24.7 Hz), 110.1 (d, $J$ = 26.0 Hz), 112.7 (d, $J$ = 4.7 Hz), 112.8 (d, $J$ = 10.1 Hz), 125.4 (d, $J$ = 10.5 Hz), 127.3, 133.5, 139.9, 146.3, 157.5 (d, $J$ = 231.9 Hz) (see Supporting Information Figure S12). MS (ESI) $m/z$: calcd for $(C_{22}H_{18}F_2N_4 + H)^+$, 347.4; found, 347.6. Anal calcd for $C_{22}H_{18}F_2N_4$ (346.3): C, 69.36; H, 3.49; N, 16.18; found: C, 69.11; H, 3.37; N, 15.93.

2,5-Bis(5-chloro-*1H*-indole-3-yl)pyrazine (**4c**) (130 mg, 68%); Mp, 278 °C. $^1$H NMR (300 MHz, DMSO-$d_6$): $\delta$ 7.21 (dd, $J$ = 2.1, 8.6 Hz, 2H), 7.50 (d, $J$ = 8.6 Hz, 2H), 8.34 (d, $J$ = 2.8 Hz, 2H), 8.51 (d, $J$ = 2.1 Hz, 2H), 9.19 (s, 2H), 11.84 (d, $J$ = 3 Hz, 2H) (see Supporting Information Figure S13). $^{13}$C NMR (75 MHz, DMSO-$d_6$): $\delta$ 112.3, 113.4, 120.7, 121.9, 124.7, 126.3, 127.1, 135.3, 140.1, 146.3 (see Supporting Information Figure S14). MS (ESI) $m/z$: calcd for $(C_{20}H_{12}Cl^{35}{}_2N_4 + H)^+$, 379.2. Found, 379.3. Anal calcd for $C_{20}H_{12}Cl_2N_4$ (378.3): C, 63.34; H, 3.19; N, 14.77; found: C, 63.09; H, 3.17; N, 14.70.


https://dx.doi.org/10.1021/acs.jmedchem.0c00826
J. Med. Chem. XXXX, XXX, XXX–XXX

**Table 5. Experimental Details of the Optimized One-Pot Masuda–Suzuki Synthesis of the Alocasin A and Hyrtinadine A Derivatives 4 by Using Methanol as a Cosolvent**

| entry | (7-aza)indole **2** [mg] ([mmol]) | heteroaryl dihalide **3** [mg] ([mmol]) | yield [mg] (%) |
|---|---|---|---|
| 1 | 432 (1.00) of 5-chloro-3-iodo-1-tosyl-1*H*-indole (**2c**) | 142 (0.50) of 5-bromo-2-iodopyrimidine (**3e**) | 177 (93) of **4j** |
| 2 | 3-iodo-5-methoxy-1-tosyl-1*H*-indole (**2a**) 427 mg/1.00 mmol | 118 (0.50) of 2,6-dibromopyridine (**3b**)118 mg (0.50) of 2,6-dibromopyridine (**3b**) | 142 (77) of **4l** |
| 3 | 3-iodo-5-fluoro-1-tosyl-1*H*-indole (**2b**) | 118 (0.50) of 2,6-dibromopyridine (**3b**) | 140 (81) of **4m** |
| 4 | 432 (1.00) of 5-chloro-3-iodo-1-tosyl-1*H*-indole (**2c**) | 118 (0.50) of 2,6-dibromopyridine (**3b**) | 160 (84) of **4n** |
| 5 | 398 (1.00) 3-iodo-1-tosyl-7-azaindol (**2g**) | 118 (0.50) of 2,6-dibromopyridine (**3b**) | 120 (90)[a] of **4p** |

[a]Even after repeated drying in vacuo at 80 °C for 42 h, dichloromethane in the crystal could not be completely removed.

2,5-Bis(5-bromo-*1H*-indole-3-yl)pyrazine (**4d**) (172 mg, 74%); Mp, 287 °C. $^1$H NMR (300 MHz, DMSO-$d_6$) $\delta$ 7.32 (dd, $J$ = 8.6, 2.0 Hz, 2H), 7.46 (dd, $J$ = 8.6, 0.6 Hz, 2H), 8.32 (d, $J$ = 2.5 Hz, 2H), 8.67 (d, $J$ = 1.9 Hz, 2H), 9.19 (s, 2H), 11.85 (s, 2H) (see Supporting Information Figure S15). $^{13}$C NMR (126 MHz, DMSO-$d_6$) $\delta$ 112.6, 113.2, 114.2, 124.0, 124.8, 127.2, 127.3, 136.0, 140.4, 146.6 (see Supporting Information Figure S16). MS (ESI) $m/z$: calcd for $(C_{20}H_{12}{}^{79}Br^{81}BrN_4 + H)^+$, 469.2; found, 469.3. Anal calcd for $C_{20}H_{12}Br_2N_4$ (468.2): C, 51.31; H, 2.58; N, 11.97; found: C, 51.04; H, 2.59; N, 11.78.

2,5-Bis(5,6-dibromo-*1H*-indole-3-yl)pyrazine (**4e**) (122 mg, 39%); Mp, >300 °C. $^1$H NMR (300 MHz, DMSO-$d_6$) $\delta$ 7.89 (s, 2H), 8.36 (d, $J$ = 2.8 Hz, 2H), 8.86 (s, 2H), 9.21 (s, 2H), 11.92 (d, $J$ = 2.4 Hz, 2H) (see Supporting Information Figure S17). $^{13}$C NMR (126 MHz, DMSO-$d_6$) $\delta$ 113.0, 115.4, 116.9, 117.5, 126.5, 127.04, 128.7, 137.5, 141.0, 146.9 (see Supporting Information Figure S18). MS (ESI) $m/z$: calcd for $(C_{20}H_{10}{}^{79}Br_2{}^{81}Br_2N_4 + H)^+$, 627.0; found, 627.1. Anal calcd for $C_{20}H_{10}Br_4N_4$ (625.9): C, 38.38; H, 1.61; N, 8.95; found: C, 38.67; H, 1.66; N, 8.86.

2,5-Bis(6-bromo-*1H*-indole-3-yl)pyrazine (**4f**) (206 mg, 88%); Mp, 284 °C. $^1$H NMR (300 MHz, DMSO-$d_6$) $\delta$ 7.29 (dd, $J$ = 8.6, 1.8 Hz, 2H), 7.67 (d, $J$ = 1.5 Hz, 2H), 8.28 (s, 2H), 8.40 (d, $J$ = 8.6 Hz, 2H), 9.14 (s, 2H), 11.77 (s, 2H) (see Supporting Information Figure S19). $^{13}$C NMR (151 MHz, DMSO-$d_6$) $\delta$ 113.2, 114.9, 115.1, 123.5, 123.6, 124.7, 127.0, 138.3, 140.6, 146.8 (see Supporting Information Figure S20). MS (ESI) $m/z$: calcd for $(C_{20}H_{12}{}^{79}Br^{81}BrN_4 + H)^+$, 469.15; found, 469.3. Anal calcd for $C_{20}H_{12}Br_2N_4$ (468.2): C, 51.31; H, 2.58; N, 11.97; found: C, 50.97; H, 2.45; N, 11.65.

2,6-Bis(5-chloro-1*H*-indole-3-yl)pyridine (**4n**) (77 mg, 41%); Mp, 241 °C. $^1$H NMR (300 MHz, DMSO-$d_6$) $\delta$ 7.19 (dd, $J$ = 8.6, 2.1 Hz, 2H), 7.50 (dd, $J$ = 8.6, 0.5 Hz, 2H), 7.64–7.59 (m, 2H), 7.76 (dd, $J$ = 8.5, 7.1 Hz, 1H), 8.19 (d, $J$ = 2.8 Hz, 2H), 8.56 (d, $J$ = 2.1 Hz, 2H), 11.73 (d, $J$ = 2.8 Hz, 2H) (see Supporting Information Figure S27). $^{13}$C NMR (75 MHz, DMSO-$d_6$) $\delta$ 113.2, 115.7, 116.1, 120.7, 121.6, 124.7, 126.3, 127.2, 135.4, 136.7, 154.0 (see Supporting Information Figure S28). MS (ESI) $m/z$: calcd for $[C_{21}H_{13}Cl^{35}{}_2N_3 + H]^+$, 378.1; found, 378.5. Anal calcd for $C_{21}H_{13}Cl_2N_3$ (378.3): C, 66.68; H, 3.46; N, 11.11; found: C, 66.69; H, 3.17; N, 10.83.

2,6-Bis(5-chloro-*1H*-indole-3-yl)pyrazine (**4r**) (124 mg, 65%); Mp, 253 °C. $^1$H NMR (600 MHz, DMSO-$d_6$) $\delta$ 7.21 (dd, $J$ = 8.6, 2.2 Hz, 2H), 7.51 (d, $J$ = 8.6 Hz, 2H), 8.34 (d, $J$ = 2.8 Hz, 2H), 8.52 (d, $J$ = 2.1 Hz, 2H), 9.19 (s, 2H), 11.85 (d, $J$ = 2.7 Hz, 2H) (see Supporting Information Figure S33). $^{13}$C NMR (151 MHz, DMSO-$d_6$) $\delta$ 112.8, 113.9, 121.2, 122.4, 125.3, 126.8, 127.6, 135.9, 140.6, 146.8 (see Supporting Information Figure S34). HR-MS (ESI) calcd for $(C_{20}H_{12}Cl^{35}{}_2N_4 + H)^+$ $m/z$, 379.0512. Found $m/z$, 379.0511. Anal calcd for $C_{20}H_{12}Cl_2N_4$ (379.24): C, 63.34; H, 3.19; N, 14.77; found: C, 63.15; H, 3.00; N, 14.66.

3,6-Bis(5-chloro-1*H*-indole-3-yl)pyridazine (**4s**) (0.143 mg, 75%); Mp, 268 °C. $^1$H NMR (600 MHz, DMSO-$d_6$) $\delta$ 7.24 (dd, $J$ = 8.6, 2.1 Hz, 2H), 7.53 (d, $J$ = 8.6 Hz, 2H), 8.13 (s, 2H), 8.37 (d, $J$ = 2.6 Hz, 2H), 8.67 (d, $J$ = 2.1 Hz, 2H), 11.91–11.87 (m, 2H) (see Supporting Information Figure S35). $^{13}$C NMR (151 MHz, DMSO-$d_6$) $\delta$ 112.9, 113.8, 121.8, 122.5, 123.9, 125.4, 126.4, 128.8, 136.0, 154.5 (see Supporting Information Figure S36). HR-MS (ESI) $m/z$: calcd for $[C_{20}H_{12}Cl^{35}{}_2N_4 + H]^+$, 379.0512; found, 379.0516. HPLC, 98.66%.

(7-Aza)indole (1.00 mmol) **2** and tetrakis(triphenylphosphane)-palladium(0) (67 mg, 0.06 mmol) were placed in a dry screw-capped vessel with a magnetic stir bar (for experimental details, see Table 5). After three cycles of evacuating and refilling with dry argon, degassed dry 1,4-dioxane (4.00 mL) was added. Then, dry triethylamine (1.40 mL, 10.0 mmol) and 4,4,5,5-tetramethyl-1,3,2-dioxaborolane (0.25 mL, 1.70 mmol) were successively added. Then, the reaction mixture was stirred in a preheated oil bath at 80 °C for 4 h. The mixture was cooled down to room temp. (water bath). Dry methanol (7.00 mL) was added, and the mixture was stirred at room temp. for 10 min. After the addition of heteroaryl dihalide **3** (0.50 mmol) and cesium carbonate (823 mg, 2.50 mmol), the mixture was stirred in a preheated oil bath at 60 °C for 18 h. After the Suzuki coupling was completed, the mixture was cooled to room temp. (water bath). Ground potassium hydroxide (140 mg, 2.50 mmol) was added, and the reaction mixture was stirred at 100 °C for 4 h. Then, after cooling to room temp. (water bath), the solvents were removed in vacuo, and the residue was adsorbed onto Celite. After purification by chromatography on silica gel (dichloromethane/methanol/aqueous ammonia, 100:1:1), the desired compounds **4** were obtained (pure according to $^1$H NMR). For further purification, trituration in dichloromethane (3 × 10 mL) by ultrasonication was necessary.

3,3′-(Pyrimidine-2,5-diyl)bis(5-chloro-1*H*-indole) (**4j**), colorless solid (177 mg, 93%); Mp, 266 °C. $^1$H NMR (DMSO-$d_6$, 600 MHz): $\delta$ = 7.21 (d, $J$ = 8.6 Hz, 2H), 7.52 (dd, $J$ = 8.5 Hz, 4.2 Hz, 2H), 7.97 (s, 1H), 8.01 (s, 1H), 8.30 (s, 1H), 8.62 (s, 1 H), 9.13 (s, 2H), 11.80 (s, 1H), 11.86 (s, 1H) (see Supporting Information Figure S21). $^{13}$C NMR (DMSO-$d_6$, 150 MHz): $\delta$ = 109.8, 114.1, 115.0, 118.8, 121.5, 122.3, 122.4, 125.3, 126.4, 127.1, 130.6, 135.8, 136.0, 154.6, 160.8 (see Supporting Information Figure S22). HR-MS (ESI) $m/z$: calcd for $[C_{20}H_{12}Cl^{35}{}_2N_4 + H]^+$, 379.0519; found, 379.0514. Anal calcd for $C_{20}H_{12}Cl_2N_4$ (379.2): C, 63.34; H, 3.19; N, 14.77; found: C, 63.15; H, 3.02; N, 14.51.

2,6-Bis(5-methoxy-1*H*-indol-3-yl)pyridine (**4l**), colorless solid (142 mg, 77%); Mp, 149 °C. $^1$H NMR (DMSO-$d_6$, 300 MHz): $\delta$ 3.67 (s, 6H), 6.82 (dd, $J$ = 8.8 Hz, 2.5 Hz, 2H), 7.36 (d, $J$ = 8.8 Hz, 2H), 7.54 (d, $J$ = 7.8 Hz, 2H), 7.72 (dd, $J$ = 8.4 Hz, 1H), 8.05 (d, $J$ = 2.8 Hz, 2H), 8.08 (d, $J$ = 2.5 Hz, 2H), 11.36 (d, $J$ = 2.9 Hz, 2H) (see Supporting Information Figure S23). $^{13}$C NMR (acetone-$d_6$,75 MHz): $\delta$ 55.8, 104.9, 113.0, 113.1, 116.6, 118.2, 126.4, 127, 133.6, 137.3, 155.8, 156.2 (see Supporting Information Figure S24). MS (ESI) $m/z$: calcd for $[C_{23}H_{19}N_3O_2 + H^+]^+$, 370.4; found, 370.3. Anal calcd for $C_{23}H_{19}N_3O_2$ (369.4): C, 74.78; H, 5.18; N, 11.37; found: C, 74.55; H, 5.34; N, 11.08.

2,6-Bis(5-fluoro-1*H*-indol-3-yl)pyridine (**4m**), colorless solid (140 mg, 81%); Mp, 227–229 °C. $^1$H NMR (DMSO-$d_6$, 300 MHz): $\delta$ 7.04 (td, $J$ = 9.1 Hz, 2.6 Hz, 2H), 7.43–7.53 (m, 2H), 7.57–7.64 (m, 2H), 7.75 (dd, $J$ = 8.4 Hz, 7.1 Hz, 1H), 8.19 (d, $J$ = 2.7 Hz, 2H), 8.24 (dd, $J$ = 10.8 Hz, 2.6 Hz, 2H), 11.60–11.73 (m, 2H) (see Supporting Information Figure S25). $^{13}$C NMR (DMSO-$d_6$, 75 MHz): $\delta$ 106.1 (d, $J$ = 24.6 Hz), 109.8 (d, $J$ = 26.1 Hz), 112.8 (d, $J$ = 9.9 Hz), 115.9, 116.26 (d, $J$ = 4.8 Hz), 125.6 (d, $J$ = 10.8 Hz), 127.6, 133.7, 136.8, 154.2, 157.6 (d, $J$ = 231.7 Hz) (see Supporting Information Figure S26). MS (ESI) $m/z$: calcd for $[C_{21}H_{13}F_2N_3 + H^+]^+$, 346.3; found, 346.3. Anal calcd for $C_{21}H_{13}F_2N_3$ (345.4): C, 73.04; H, 3.79; N, 12.17; found: C, 73.06; H, 4.03; N, 11.94.


https://dx.doi.org/10.1021/acs.jmedchem.0c00826
J. Med. Chem. XXXX, XXX, XXX–XXX

2,6-Bis(5-chloro-1*H*-indol-3-yl)pyridine (**4n**), colorless solid (160 mg, 84%). Mp, 241 °C. $^1$H NMR (DMSO-$d_6$, 600 MHz): $\delta$ = 7.19 (dd, $J$ = 8.6 Hz, 2.1 Hz, 2H), 7.50 (d, $J$ = 8.6 Hz, 2H), 7.61 (d, $J$ = 7.8 Hz, 2H), 7.76 (t, $J$ = 7.8 Hz, 1H), 8.18 (d, $J$ = 2.7 Hz, 2H), 8.56 (d, $J$ = 2.0 Hz, 2H), 11.73 (s, 2H) (see Supporting Information Figure S27). $^{13}$C NMR (DMSO-$d_6$, 150 MHz): $\delta$ = 113.8, 116.7, 121.2, 122.2, 125.3, 126.8, 127.8, 135.9 (see Supporting Information Figure S28). HR-MS (ESI) $m/z$: calcd for $[C_{21}H_{13}Cl^{35}{}_2N_3 + H]^+$, 378.0559; found, 378.0562. Anal calcd for $C_{21}H_{12}Cl_2N_3$ (378.3): C, 66.68; H, 3.46; N, 11.11; found: C, 66.53; H, 3.35; N, 10.84.

2,6-Bis(1*H*-pyrrolo[2,3-*b*]pyridin-3-yl)pyridine (**4p**), light yellow solid (120 mg, 90%). $^1$H NMR (DMSO-$d_6$, 600 MHz): $\delta$ = 7.21 (dd, $J$ = 4.6, 7.9 Hz, 2H), 7.68 (d, $J$ = 7.8 Hz, 2H), 7.80 (t, $J$ = 7.8 Hz, 1H), 8.27 (d, $J$ = 2.6 Hz, 2H), 8.31 (dd, $J$ = 4.6 Hz, 1.5 Hz, 2H), 8.77 (dd, $J$ = 7.9 Hz, 1.5 Hz, 2H), 12.07 (s, 2H) (see Supporting Information Figure S29). $^{13}$C NMR (DMSO-$d_6$, 150 MHz): $\delta$ = 115.2, 116.8, 116.9, 118.1, 126.5, 129.9, 137.5, 143.5, 149.7, 154.4 (see Supporting Information Figure S30). Anal calcd for $C_{19}H_{13}N_5$ + 0.08 $CH_2Cl_2$ (311.3 + 6.79): C, 71.56; H, 4.15; N, 21.83; found: C, 71.16; H, 4.05; N, 21.51.

Indole **2** (1.00 mmol) and tetrakis(triphenylphosphane)-palladium(0) (67 mg, 0.06 mmol) were placed in a dry screw-capped vessel with a magnetic stir bar (for experimental details, see Table 6).

**Table 6. Experimental Details of the Optimized One-Pot Masuda–Suzuki Synthesis of the Alocasin A and Hyrtinadine A Derivatives 4 by Using Water as a Cosolvent**

| entry | indole **2** [mg] ([mmol]) | heteroaryl dihalide **3** [mg] ([mmol]) | yield [mg] (%) |
|---|---|---|---|
| 1 | 432 (1.00) of 5-chloro-3-iodo-1-tosyl-1*H*-indole (**2c**) | 142 (0.50) of 5-bromo-2-iodopyrimidine (**3e**) | 150 (80) of **4j** |
| 2 | 432 (1.00) of 5-chloro-3-iodo-1-tosyl-1*H*-indole (**2c**) | 118 (0.50) of 2,6-dibromopyridine (**3b**) | 160 (84) of **4n** |
| 3 | 432 (1.00) of 5-chloro-3-iodo-1-tosyl-1*H*-indole (**2c**) | 75 (0.50) of 2,4-dichloropyrimidine (**3f**) | 110 (58) of **4q** |
| 4 | 397 (1.00) of 3-iodo-1-tosyl-1*H*-indole (**2h**) | 118 (0.50) of 3,5-dibromopyridine (**3g**) | 66 (43) of **4u** |
| 5 | 415 (1.00) of 3-iodo-5-fluoro-1-tosyl-1*H*-indole (**2b**) | 118 (0.50) of 3,5-dibromopyridine (**3g**) | 120 (70) of **4v** |

After three cycles of evacuating and refilling with dry argon, degassed dry 1,4-dioxane (4.00 mL) was added. Then, dry triethylamine (1.40 mL, 10.0 mmol) and 4,4,5,5-tetramethyl-1,3,2-dioxaborolane (0.25 mL, 1.70 mmol) were successively added. Then, the reaction mixture was stirred in a preheated oil bath at 80 °C for 4 h. The mixture was cooled down to room temp. (water bath). Distilled water (3.00 mL) was added, and the mixture was stirred at room temp. for 10 min. After the addition of heteroaryl dihalide **3** (0.50 mmol) and cesium carbonate (823 mg, 2.50 mmol), the mixture was stirred in a preheated oil bath at 60 °C for 42 h. After the Suzuki coupling was completed, the mixture was cooled to room temp. (water bath). Methanol (4.00 mL) and ground potassium hydroxide (140 mg, 2.50 mmol) were added, and the reaction was stirred at 100 °C for 5 h. Then, after cooling to room temp. (water bath), the solvents were removed in vacuo, and the residue was adsorbed onto Celite. After purification by chromatography on silica gel (dichloromethane/methanol/aqueous ammonia, 100:1:1), the desired compounds **4** were obtained in a pure form. For removing residual solvents from chromatography, compounds were triturated in *n*-hexane under ultrasonication.

3,3′-(Pyrimidine-2,5-diyl)bis(5-chloro-1*H*-indole) (**4j**), colorless solid (150 mg, 80%). Mp, 266 °C. $^1$H NMR (DMSO-$d_6$, 600 MHz): $\delta$ = 7.21 (d, $J$ = 8.6 Hz, 2H), 7.52 (dd, $J$ = 8.5 Hz, 4.2 Hz, 2H), 7.97 (s, 1H), 8.01 (s, 1H), 8.30 (s, 1H), 8.62 (s, 1H), 9.13 (s, 2H), 11.80 (s, 1H), 11.86 (s, 1H) (see Supporting Information Figure S21). $^{13}$C NMR (DMSO-$d_6$, 150 MHz): $\delta$ = 109.8, 114.1, 115.0, 118.8, 121.5, 122.3, 122.4, 125.3, 126.4, 127.1, 130.6, 135.8, 136.0, 154.6, 160.8 (see Supporting Information Figure S22). ESI MS ($m/z$ (%)): 401 (12) $[M(Cl^{35}) + Na]^+$, 379 (100) $[M(Cl^{35}) + H]^+$. Anal calcd for $C_{20}H_{12}Cl_2N_4$ (379.2): C, 63.34; H, 3.19; N, 14.17; found: C, 63.18; H, 3.47; N, 14.47.

2,6-Bis(5-chloro-1*H*-indol-3-yl)pyridine (**4n**), colorless solid (146 mg, 77%). Mp, 241 °C. $^1$H NMR (DMSO-$d_6$, 600 MHz): $\delta$ = 7.19 (dd, $J$ = 8.6 Hz, 2.1 Hz, 2H), 7.50 (d, $J$ = 8.6 Hz, 2H), 7.61 (d, $J$ = 7.8 Hz, 2H), 7.76 (t, $J$ = 7.8 Hz, 1H), 8.18 (d, $J$ = 2.7 Hz, 2H), 8.56 (d, $J$ = 2.0 Hz, 2H), 11.73 (s, 2H) (see Supporting Information Figure S27). $^{13}$C NMR (DMSO-$d_6$, 150 MHz): $\delta$ = 113.8, 116.3, 116.7, 121.2, 122.2, 125.3, 126.8, 127.8, 135.9, 137.3, 154.6 (see Supporting Information Figure S28). Anal calcd for $C_{21}H_{13}Cl_2N_3$ (378.3): C, 66.68; H, 3.46; N, 11.11; found: C, 66.39; H, 3.43; N, 10.90.

3,3′-(Pyrimidine-2,4-diyl)bis(5-chloro-1*H*-indole) (**4q**), colorless solid (110 mg, 58%). Mp, 225 °C. $^1$H NMR (DMSO-$d_6$, 600 MHz): $\delta$ = 7.22 (dd, $J$ = 8.6 Hz, 2.1 Hz, 1H), 7.26 (dd, $J$ = 8.6 Hz, 2.0 Hz, 1H), 7.54 (t, $J$ = 8.1 Hz, 2H), 7.62 (d, $J$ = 5.4 Hz, 1H), 8.31 (d, $J$ = 2.7 Hz, 1H), 8.48 (d, $J$ = 2.8 Hz, 1H), 8.62 (d, $J$ = 2.0 Hz, 1H$_r$), 8.65 (d, $J$ = 1.9 Hz, 1H), 8.67 (d, $J$ = 5.4 Hz, 1H), 11.90 (s, 1H), 12.06 (s, 1H) (see Supporting Information Figure S31). $^{13}$C NMR (DMSO-$d_6$, 150 MHz): $\delta$ = 112.7, 113.8, 114.1, 114.2, 115.7, 121.3, 121.4, 122.4, 122.7, 125.6, 126.0, 126.7, 127.2, 130.6, 131.0, 136.0, 136.1, 156.9, 161.6, 163.4 (see Supporting Information Figure S32). MS (ESI) $m/z$: calcd for $[C_{20}H_{12}Cl^{35}{}_2N_4 + H]^+$, 380.3; found, 380.5. Anal calcd for $C_{20}H_{12}Cl_2N_4$ (379.2): C, 63.34; H, 3.19; N, 14.77; found: C, 63.35; H, 3.04; N, 14.51.

3,5-Bis(1*H*-indol-3-yl)pyridine (**4u**), colorless solid (66 mg, 43%). Mp, 324 °C. $^1$H NMR (DMSO-$d_6$, 600 MHz): $\delta$ = 7.15 (t, $J$ = 7.1 Hz, 2H), 7.20 (t, $J$ = 7.1 Hz, 2H), 7.50 (d, $J$ = 8.0 Hz, 2H), 7.88–7.97 (m, 4H), 8.28 (t, $J$ = 2.0 Hz, 1H), 8.79 (d, $J$ = 1.9 Hz, 2H), 11.55 (s, 2H) (see Supporting Information Figure S37). $^{13}$C NMR (DMSO-$d_6$, 75 MHz): $\delta$ = 112.2, 112.4, 118.9, 120.1, 121.8, 124.5, 125.0, 130.7, 131.8, 137.0, 144.3. (see Supporting Information Figure S38). HR-MS (ESI) calcd for $[C_{21}H_{15}N_3 + H]^+$ $m/z$, 310.1339. Found $m/z$, 310.1342.

3,5-Bis(5-fluoro-1*H*-indol-3-yl)pyridine (**4v**), light yellow solid (120 mg, 70%). Mp, 293 °C. $^1$H NMR (DMSO-$d_6$, 600 MHz): $\delta$ = 7.05 (td, $J$ = 9.1 Hz, 2.5 Hz, 2H), 7.50 (dd, $J$ = 8.8 Hz, 4.7 Hz, 2H), 7.65 (dd, $J$ = 10.3 Hz, 2.5 Hz, 2H), 8.02 (d, $J$ = 2.7 Hz, 2H), 8.21 (t, $J$ = 2.2 Hz, 1H), 8.78 (d, $J$ = 2.1 Hz, 2H), 11.66 (s, 2H) (see Supporting Information Figure S39). $^{13}$C NMR (DMSO-$d_6$, 75 MHz): $\delta$ = 103.7 (d, $J$ = 23.9 Hz), 109.9 (d, $J$ = 25.9 Hz), 112.6 (d, $J$ = 4.7 Hz), 113.2 (d, $J$ = 9.9 Hz), 125.0 (d, $J$ = 10.0 Hz), 126.6, 130.4, 131.3, 133.6, 144.2, 157.6 (d, $J$ = 232.2 Hz) (see Supporting Information Figure S40). HR-MS (ESI) calcd for $[C_{21}H_{13}F_2N_3 + H]^+$ $m/z$, 346.1150. Found $m/z$, 346.1155.

**Solubility Tests.** Compounds **4c**, **4d**, and **4r** as well as the *in vivo* tested compounds **4j** and **4n** have been tested for solubility in DMSO

**Table 7. Absorption Coefficients $\varepsilon$ for 4c, 4d, 4r, 4j, and 4n in DMSO**

| coefficients | compound | | | | |
|---|---|---|---|---|---|
| | **4c** | **4d** | **4j** | **4n** | **4r** |
| $\lambda_{max,abs}$ [nm] | 375 | 376 | 339 | 332 | 365 |
| extinction coefficient $\varepsilon$ [L·mol$^{-1}$·cm$^{-1}$] | 8000 | 7200 | 11,700 | 5800 | 3900 |
| $r^2$ | 0.98658 | 0.9934 | 0.99442 | 0.95684 | 0.92262 |


https://dx.doi.org/10.1021/acs.jmedchem.0c00826
J. Med. Chem. XXXX, XXX, XXX–XXX

Table 8. Absorption Coefficients $\epsilon$ for 4c, 4d, 4r, 4j, and 4n in DMSO/PBS Buffer (30:70 to 40:60, pH = 7.77)

| coefficients | compound | | | | |
|---|---|---|---|---|---|
| | 4c | 4d | 4j | 4n | 4r |
| $\lambda_{max,abs}$ [nm] | 377 | 377 | 337 | 328 | 367 |
| extinction coefficient $\epsilon$ [L·mol$^{-1}$·cm$^{-1}$] | 6000 | 5200 | 7900 | 4700 | 5300 |
| $r^2$ | 0.99776 | 0.99837 | 0.97886 | 0.99785 | 0.99751 |

and PBS buffer. The longest wavelength absorption bands of the compounds were investigated at different concentrations $c$, and the absorption coefficients $\epsilon$ were determined (Tables 7 and 8). If the compounds are completely dissolved, then the Lambert−Beer law ($A = \epsilon_\lambda \times c \times d$) is fulfilled.

**Stability Study.** To investigate the stability of compound **4c**, absorption spectra of **4c** were measured at different times in DMSO/PBS buffer (40:60, pH = 7.77) at a concentration of 0.19 $\mu$M. Absorption maxima of **4c** were determined and plotted over time to observe potential degradation or aggregation.

**Biological Evaluation.** *Bacterial Strains.* Nosocomial bacterial reference strains were cultivated in a Mueller Hinton medium at 37 °C and included different strains of *Staphylococcus aureus* (MSSA strain ATCC 25923, MRSA/VISA strain ATCC 700699, MRSA strain LAC USA300, and pyruvate kinase-deficient MRSA strain LAC Δ*pyk*::Erm$^R$ (the latter was obtained from the laboratory of Anthony R. Richardson, Department of Microbiology and Immunology, School of Medicine, University of North Carolina at Chapel Hill, Chapel Hill, NC, USA[34])), *Enterococcus faecalis* (ATCC 29212, ATCC 51299 (gentamycin-resistant)), *Enterococcus faecium* (ATCC 35667, ATCC 700221 (vancomycin-resistant)), and *Acinetobacter baumannii* (ATCC BAA 1605). *Mycobacterium tuberculosis* strain H37Rv was grown aerobically in a Middlebrook 7H9 medium supplemented with 10% (v/v) ADS enrichment (5% w/v, bovine serum albumin fraction V; 2% w/v, glucose; 0.85% w/v, sodium chloride), 0.5% (v/v) glycerol, and 0.05% (v/v) tyloxapol at 37 °C.

*Determination of Minimal Inhibitory Concentration (MIC).* All compounds **c** were tested for their antibacterial activities against various pathogenic bacterial strains including nosocomial pathogens and *Mycobacterium tuberculosis*. For the tested nosocomial pathogens (*S. aureus*, *E. faecalis*, *E. faecium*, and *A. baumannii*), the broth microdilution method according to the recommendations of the Clinical and Laboratory Standards Institute (CLSI) (CLSI M7-A9, 2012) was used. Briefly, bacterial cells were grown aerobically in a Mueller Hinton (MH) medium at 37 °C and 180 rpm. A preculture was grown until the log phase ($OD_{600\ nm} \sim 0.5$) and then seeded at 5 × 10$^4$ CFU/well in a total volume of 100 $\mu$L in 96 well round bottom microtiter plates and incubated with serially diluted test substances **4** at a concentration range of 100−0.78 $\mu$M. Microplates were incubated aerobically at 37 °C for 24 h. MICs were determined macroscopically by identifying the minimum concentration of the compounds **4** that led to complete inhibition of visual growth of the bacteria.

The MICs of compounds **4c**, **4d**, **4j**, **4n**, **4q**, and **4s** were additionally quantified via the BacTiter-Glo assay (Promega, Madison, WI, USA). Briefly, after an incubation time of 24 h, each well was resuspended by pipetting, and 50 $\mu$L aliquots were transferred into an opaque-walled multiwell plate. Additionally, control wells containing a medium without cells to determine background luminescence were prepared. A BacTiter-Glo reagent (50 $\mu$L) was added to each well. Contents were mixed and incubated for five minutes at room temperature. Luminescence was measured using a microplate reader. Growth was calculated relative to the background luminescence (0% growth) and a DMSO solvent control (100% growth).

The influence of glucose or pyruvate as a carbon source on drug susceptibility of *S. aureus* cells was determined in a minimal medium. MIC of active compounds **4** was determined in two-fold serial dilutions ranging from 0.15 to 25 $\mu$M in a minimal medium M9 (1 × M9 salts, 2 mM $MgSO_4$, 0.1 mM $CaCl_2$, 0.05 mM nicotinamide, and 0.125% w/v casamino acids) with either 1% glucose or pyruvate. 5 × 10$^4$ CFU/well was seeded in a total volume of 100 $\mu$L into 96 well round bottom microtiter plates and incubated aerobically at 37 °C for 24 h. MICs were determined by using the resazurin dye reduction assay as described below for *M. tuberculosis*.

For the determination of MIC against *M. tuberculosis*, bacteria were precultured until the log phase ($OD_{600\ nm} = 0.5-1$) and then seeded at 1 × 10$^5$ cells per well in a total volume of 100 $\mu$L in 96 well round bottom microtiter plates and incubated with serially diluted test compounds **4** at a concentration range of 100−0.78 $\mu$M. Microplates were incubated at 37 °C for five days. Afterward, 10 $\mu$L/well of a 100 $\mu$g/mL resazurin solution was added and incubated at ambient temperature for further 16 h. Then, cells were fixed for 30 min after formalin addition (5% v/v, final concentration). For viability determination, fluorescence was quantified using a microplate reader (excitation, 540 nm; emission, 590 nm). Percentage of growth was calculated relative to rifampicin-treated (0% growth) and DMSO-treated (100% growth) controls.

*Evaluation of Compound Interaction via Checkerboard Assay.* The fractional inhibitory concentration index (FICI) of bisindoles in combination with colistin was determined in a 96 well plate employing two-dimensional dilutions of bioactive agents. Both compounds were serially diluted in a 2-fold manner. Colistin was diluted horizontally from 3.13 to 0.025 $\mu$M, while **4j** or **4n** was diluted vertically from 100 to 0.78 $\mu$M. Respective exponential growth phase cultures of test Gram-negative bacteria were adjusted and seeded at 5 × 10$^4$ CFU/well in a total volume of 100 $\mu$L and incubated for 24 h, at 37 °C. Upon incubation, resazurin was used as a viability marker. The FICI was calculated as the sum of the quotients of the MICs of each compound when used in combination (A and B) and the MIC of the compound alone ($MIC_A$ and $MIC_B$, respectively)

$$\mathrm{FICI}(A+B) = \frac{A}{\mathrm{MIC_A}} + \frac{B}{\mathrm{MIC_B}}$$

Total synergism and antagonism between bisindoles and colistin were defined as FICI ≤ 0.5 and > 2, respectively. Partial synergism was defined by 0.5 < FICI ≤ 0.75, while an indifferent or additive effect was denoted by 0.75 < FICI ≤ 2.[40]

*Determination of the Cytotoxicity and Therapeutic Index.* The cytotoxicity of compounds **4c**, **4d**, **4j**, **4n**, **4q**, and **4s** was determined *in vitro* using the human monocyte cell line THP-1 (Deutsche Sammlung von Mikroorganismen und Zellkulturen GmbH, DSM) and the human fetal lung fibroblast cell line MRC-5 (American Type Culture Collection, ATCC). Compounds **4j**, **4n**, and **4q** were additionally tested against the human kidney cell line HEK293, the human hepatocellular carcinoma cell line HepG2, and the lung carcinoma cell line CLS-54 (all obtained from CLS Cell Lines Service GmbH). THP-1 and CLS-54 cells were cultured in an RPMI 1640 medium containing 10% (v/v) fetal bovine serum (FBS). MRC-5 cells were incubated in Dulbecco's modified Eagle medium (DMEM) containing 10% (v/v) FBS. HEK293 cells were cultivated using an EMEM medium supplemented with 2 mM L-glutamine, 1% (v/v) non-essential amino acids, 1 mM sodium pyruvate, and 10% (v/v) FBS. HepG2 cells were cultivated using Ham's F12 medium supplemented with 2 mM L-glutamine and 10% (v/v) FBS. All cells were cultivated at 37 °C in a humidified atmosphere of 5% $CO_2$. Cells were seeded at approx. 5 × 10$^4$ cells/well in a total volume of 100 $\mu$L in 96 well flat bottom microtiter plates containing two-fold serially diluted test compounds **4** at a maximum final concentration of 100 $\mu$M. Cells treated with DMSO in a final concentration of 1% (v/v) were used as solvent controls. After an incubation time of 48 h, 10 $\mu$L of resazurin solution (100 $\mu$g/mL) was added per well and incubated for further 3 h at 37 °C in a humidified atmosphere of 5% $CO_2$.


https://dx.doi.org/10.1021/acs.jmedchem.0c00826
J. Med. Chem. XXXX, XXX, XXX−XXX

Fluorescence was quantified using a microplate reader (excitation, 540 nm; emission, 590 nm). Growth was calculated relative to non-inoculated (i.e., cell-free) (0% growth) and untreated (100% growth) controls in triplicate experiments.

For determination of the therapeutic index of the tested substances **4**, the selectivity index (SI) was determined by the quotient of the observed cytotoxic concentration reducing growth by 50% (IC50) and MIC. Compounds **4** with SI ≥ 10 were characterized in further experiments.

*Testing for Hemolytic Activity.* Defibrinated sheep red blood cells (RBC) purchased from Thermo Fisher Scientific, Germany were washed thrice with PBS (3000 rpm, 10 min at 4 °C) and then diluted in PBS to obtain an 8% RBC suspension. 100 μL RBC suspensions were treated with 100 μL of compounds **4j** and **4n** at the indicated final concentrations and incubated at 37 °C. Triton X-100 (2%) and PBS served as positive and negative controls, respectively. After 1 h incubation, the mixtures were collected and centrifuged at 3000 rpm for 3 min. The supernatant (100 μL) was transferred to a new 96 well microtiter plate, and hemoglobin release was measured in a Tecan Infinite 200pro plate reader by absorption at 540 nm.

*Determination of Time-Kill Curves In Vitro.* Killing kinetics were measured for compounds **4c**, **4d**, **4j**, **4n**, **4q**, and **4s** against the *S. aureus* MRSA/VISA strain ATCC 700699. An overnight culture of the strain was adjusted to a final inoculum concentration of $10^6$ CFU/mL cultivated in MH broth containing the tested compounds **4** at five-fold MIC. Cultures containing moxifloxacin at five-fold MIC (20 μM) were used as a positive control. Furthermore, MRSA cultures cultivated in MH broth with 0.02% DMSO, correlating to the maximum amount of DMSO in the compound containing cultures, were handled as an antibiotic-free control. In a second attempt, the culture medium was removed after 6 h post-exposure to compounds **4** and replaced by a fresh compound-containing medium. This should overcome limited antibacterial activity in the case that compound **4** was degraded or consumed during the experiment. Therefore, the culture was centrifuged at 4000 rpm for 10 min. Afterward, the bacterial cell pellet was washed in PBS and suspended in a fresh medium containing the corresponding compound **4** at the initial concentration. Shaking cultures were incubated for 24 h at 37 °C at 180 rpm. After 0, 3, 6, and 24 h of incubation, viability, expressed as CFU/mL, was determined by plating 100 μL aliquots of a serial dilution onto MH agar plates. The plates were incubated aerobically at 37 °C for 24 h before colonies were counted.

For determination of the influence of the carbon source on the killing effect, *S. aureus* LAC WT and LAC Δ*pyk*::$Erm^R$ were cultivated in TSB broth without glucose with 1% sodium pyruvate and treated like described elsewhere.[34]

*In Vivo Efficacy Studies in a Mouse Wound Infection Model.* The *in vivo* efficacy of bisindoles was investigated in a mouse skin infection model. BALB/c female mice were anesthetized with 4% chloral hydrate (0.1 mL/10 g), and 10 mm diameter wounds in the backs were achieved using surgical punches. Subsequently, a suspension containing $1 \times 10^7$ CFU of MRSA strain T144 in PBS was inoculated onto each wound. At 1 h post-infection, PBS (vehicle), **4j** (5 mg/kg), **4n** (5 mg/kg), and vancomycin (20 mg/kg) were topically administered to the wound in a single-dose treatment. The gross and microscopic appearance of the skin surface was monitored daily for 12 days. At the end of the experiment, the wound skin was excised for homogenization to count the bacterial loads of MRSA in the skin employing CFU plating. All animal experiments were approved by the Institutional Animal Care and Use Committee of the China Agricultural University.

*In Vivo Efficacy Studies in a Mouse Peritonitis-Sepsis Model.* BALB/c female mice ($n$ = 6 per group) were infected with 0.5 mL of an MRSA T144 suspension ($5 \times 10^8$ CFU per mouse) via intraperitoneal injection. At 1 h post-infection, all mice were treated with either PBS (vehicle), **4j** (5 mg/kg), or **4n** (5 mg/kg) at single intraperitoneal doses. Vancomycin at a single dose of 20 mg/kg was used as a positive control. The survival rates of treated mice were recorded during a period of 48 h. All animal experiments were approved by the Institutional Animal Care and Use Committee of the China Agricultural University.

*Expression and Purification of Recombinant MRSA Pyruvate Kinase (PK).* The *pyk* gene was amplified by PCR using genomic DNA of *S. aureus* ATCC700699 as the template and employing the oligonucleotides (restriction sites are underlined) 5′His6N_NcoI_pyk (5′-TTTTTCCATGGATGCATCATCATCATCATCATAGAAAAACTAAAATTGTA-3′) introducing an N-terminal His6 tag and 3′_XhoI_pyk (5′-TTTTTCTCGAGTTATAGTACGTTTGCATATCCT-3′). The resulting PCR fragment was cloned into the expression vector pET28a(+) using the restriction sites *Nco*I and *Xho*I, and the resulting plasmid pET28a(kan)::His6N-pyk was used to express recombinant PK in *E. coli* NiCo21(DE3). Cells were grown in a YT medium (16 g/L tryptone, 10 g/L yeast extract, and 5 g/L NaCl) at 37 °C with shaking at 180 rpm until an $OD_{600\ nm}$ of approximately 0.6 was reached, then induced by addition of 0.1 mM isopropyl-β-D-thiogalactopyranoside (IPTG), and incubated at 20 °C and 50 rpm for further 24 h. Subsequently, cells were harvested by centrifugation, resuspended in lysis buffer (50 mM TRIS-HCl, (pH 7.5), 100 mM KCl, 10 mM $MgCl_2$, 200 mM NaCl, 10 mM imidazole, 0.5% (v/v) Triton-X100, 0.5 mM (v/v) DTT, and 10% (v/v) glycerol) containing a 1 mg/mL lysozyme and a 10 μg/mL protease inhibitor and lysed by sonicating on ice for 1.5 min. Cell lysates were cleared by centrifuging for 30 min at 16,000*g* and 4 °C. A Ni-NTA agarose suspension (3 mL) was washed twice with 3 mL of lysis buffer, mixed with the cleared lysate for batch binding, and rotated gently on ice for 1 h to allow histidine-tagged proteins to bind. A Pierce disposable column with a porous polyethylene disc was washed with lysis buffer followed by adding the Ni-NTA-lysate suspension to the column. The column resin was washed with 10 column volumes of lysis buffer containing 30 mM imidazole. His-tagged proteins were then eluted with lysis buffer containing 300 mM imidazole and concentrated with a Vivaspin 20 centrifugal concentrator (MWCO 10 kDa). Finally, the protein sample was desalted by using the PD MidiTrap G-10 columns employing exchange buffer (30 mM TRIS-HCl (pH 7.5), 25 mM KCl, 5 mM $MgCl_2$, and 10% (v/v) glycerol). SDS-polyacrylamide gel electrophoresis (PAGE) and Coomassie staining were used to evaluate the protein's purity, while its concentration was determined by BCA assay.

*Measuring of Pyruvate Kinase Activity.* To evaluate the potential of bisindoles **4** to impair enzymatic activity of MRSA PK, activities of PKs from rabbit muscle and from MRSA were measured via a lactate-dehydrogenase (LDH)-linked assay by measuring the consumption of NADH essentially as described previously.[33] PK activity was assayed using black, flat bottom μCLEAR 96 well plates in a total volume of 200 μL in a reaction mixture containing 60 mM HEPES (pH 7.5), 67 mM KCl, 6.7 mM $MgSO_4$, 1.5 mM ADP, 1.5 mM ribose-5-phosphate, 1.5 mM phosphoenolpyruvate, 0.22 mM NADH, and 5 U/mL LDH. Bisindoles **4** were added at various concentrations as indicated. The reaction was initiated by adding 5 μg of respective PKs, incubated at 30 °C, and quantified by measuring absorbance at 340 nm for 5 min using an Infinite M Plex Tecan reader. Inhibitor concentrations higher than 12.5 μM were not tested as the tested compounds **4** interfered with absorbance at 340 nm under these conditions. PK activity, expressed as initial velocity in μmol/min/mg protein, is defined as the amount of PK that catalyzes the formation of 1 μmol of product per minute and was calculated as: $v$ (μmol/min/mg protein) = [(Δ$E$/min)/(ε × $d$)/mL]/mg protein, where Δ$E$ = change of extinction per minute; mL = reaction volume (0.2 mL); ε = extinction coefficient of NADH (6.22 $mM^{-1}$ $cm^{-1}$); $d$ = path of light (0.64 cm). The resulting curve was fitted by nonlinear regression to the allosteric sigmoidal kinetic model of GraphPad Prism 5 software.

*Fluorescence Microscopy.* Fluorescence microscopy was done as described in a previous study with some modifications.[41] Briefly, cells of methicillin-susceptible *S. aureus* strain ATCC 29213 grown and adjusted to a cell density of 0.3 $OD_{600\ nm}$ were incubated with 5-fold MIC of **4n** in an MH medium for 30 min at 37 °C and 150 rpm. Upon incubation, cells were pelleted (3000 g for 15 min), washed with PBS, and then incubated with PI (7.5 μg/mL in water) in the dark for 15 min at 0−4 °C. PI-incubated cells were then washed three


https://dx.doi.org/10.1021/acs.jmedchem.0c00826
J. Med. Chem. XXXX, XXX, XXX−XXX

times with PBS to remove excess PI and further incubated with DAPI (10 μg/mL in water) in the dark for 15 min at 0−4 °C. After three washing steps of removing excess DAPI, cells were fixed by resuspending pellets in 4% paraformaldehyde (pH 6.9) and incubated at room temperature for 20 min. Fixed bacterial pellets were washed, suspended in PBS, and examined via the oil-immersion objective (40×) of a Nikon Eclipse TS100 fluorescence microscope.

*Propidium Iodide Internalization Assay.* An actively growing *S. aureus* culture was washed, harvested, and resuspended in PBS supplemented with 1% glucose. Suspended culture was adjusted to $OD_{600\ nm}$ = 0.4 and then incubated with 7.5 μg/mL PI for 10 min at 37 °C. PI-incubated cells (100 μL) were dispensed in a black walled 96 well plate, and baseline fluorescence (excitation, 535 nm; emission, 617 nm) was established for 10 min. Cells were then treated with 100 μL of 10-fold MIC of **4n** (final concentration = 5-fold MIC). Lysostaphin was used as a positive control, while linezolid, daptomycin, moxifloxacin, and DMSO served as negative controls. Using a Tecan Infinite M Plex plate reader, fluorescence intensity of the PI dye was measured every 5 min for 2 h at 535 nm excitation wavelength and 617 nm emission wavelength.[42]

*ATP and GFP Release.* To determine the leakage of adenosine triphosphate (ATP) and green fluorescent protein (GFP) at intervals upon compound treatment, cells of recombinant *S. aureus* strain ATCC 700699 expressing GFP were washed and suspended in PBS supplemented with 1% glucose and then adjusted to 0.5 $OD_{600\ nm}$. The adjusted culture was incubated with 5-fold MIC of **4n** at 37 °C and 150 rpm. At different time points (0, 0.5, 1, 3, and 6 h), samples were collected and centrifuged at 4 °C, 10,000*g* for 10 min. The ATP present in the cell-free supernatants was then quantified using a BacTiter-Glo assay kit (Promega, Madison, WI, USA). For GFP, 100 μL of cell-free supernatants was dispensed in triplicates in a black walled 96 well plate, and GFP fluorescence (excitation wavelength, 475 nm; emission wavelength, 509 nm) was measured using a Tecan Infinite M Plex plate reader. Lysostaphin served as a positive control, while DMSO and moxifloxacin were negative controls for both experiments.[42]

*Assessment of Cell Lysis.* Cells of *S. aureus* strain ATCC 700699 cultivated in a Mueller Hinton medium until the mid-exponential phase were adjusted to $OD_{600\ nm}$ ∼ 0.3 and incubated at 37 °C with 8-fold MIC of compounds for 2 h. At different time points (0, 30, 60, 90, and 120 min), turbidity of individual cultures was monitored by measuring the optical densities of samples collected from each bacterial culture at 600 nm using a photometer. Decrease in turbidity is indicative of cell lysis.

*Isolation of Genomic DNA.* For isolation of the genomic DNA, individual resistant mutants were cultivated overnight. Bacterial suspensions were centrifuged at 4000 rpm for 5 min. Afterward, bacterial cell pellets were suspended in a lysostaphin-GTE solution (200 μg/mL lysostaphin in 25 mM Tris-Cl, pH 8.0; 10 mM EDTA; 50 mM glucose) and incubated at 37 °C for 30 min. After addition of 5 μL of proteinase K (10 mg/mL), the suspensions were incubated at 65 °C for 1 h. Subsequently, an equal volume of 24:1 chloroform/isoamyl alcohol was added. The mixture was shaken vigorously and spun at 4000 rpm for 10 min. The aqueous layer was transferred in a fresh tube, and the extraction step was repeated. DNA was precipitated by addition of 60 μL of NaCl (5 M) and 1 mL of ethanol. After centrifugation and aspiration of the supernatant, the DNA pellet was air-dried for 15 min. Finally, the DNA was dissolved in TE buffer containing RNAse (10 mM Tris, 0.1 mM EDTA, and pH 7.4).

*Whole Genome Sequencing.* Genomic DNA samples of four MRSA mutants used for genome sequencing were quantified by photometric measurement using a NanoDrop One device (Thermo Fisher Scientific, Inc.), and quality was measured by capillary electrophoresis using the Fragment Analyzer and the "High Sensitivity Genomic DNA Assay" (Agilent Technologies, Inc.). Library preparation was performed according to manufacturer's protocol using a TruePrep DNA Library Prep Kit V2 for Illumina (1 ng) (Vazyme Biotech Co., Ltd.). Libraries were normalized to 4 nM and pooled and subsequently sequenced on a MiSeq system (Illumina, Inc.) with a read setup of 2x251 bp. Base calling was performed using Casava software, v1.8. The reads were assembled using a comparative genome assembly method and compared with the parent methicillin-resistant *S. aureus* genome (strain ATCC 700699 = Mu50; GenBank accession GCA_000009665.1). The mean depth of coverage ranged from 69× to 114×. Sequencing was performed at the Biological and Medical Research Center, Genomics and Transcriptomics Laboratory, Heinrich Heine University Düsseldorf, Düsseldorf, Germany.

## ■ ASSOCIATED CONTENT

### Supporting Information

The Supporting Information is available free of charge at https://pubs.acs.org/doi/10.1021/acs.jmedchem.0c00826.

MICs of compounds **4** against all tested bacteria strains (Table S1); cytotoxicity data of compounds **4j**, **4n**, and **4q** against the human cell lines HEK293, HepG2, and CLS-54 (Table S2); SNPs present in MRSA resistant mutants (Table S3); MICs of compounds of different classes against MRSA resistant mutants and wild-type (Table S4); dose−response curve of compound **4r** against MRSA (Figure S1); solubility assessment of compounds **4c**, **4d**, **4j**, **4n**, and **4r** (Figure S2); absorption maxima of compounds **4c**, **4d**, **4j**, **4n**, and **4r** (Figure S3); hemolytic activity of **4j** and **4n** on sheep red blood cells (Figure S4); stability evaluation of compound **4c** (Figure S5); dose−response curves for **4d**, **4n**, **4q**, and **4s** against MRSA LAC WT and LAC Δ*pyk*::$Erm^R$ in minimal medium M9 (Figure S6); studies describing optimization of reaction conditions (Scheme S1 and Table S5); analytical data of compounds **1a**, **4a**−**4f**, **4j**, **4l**−**4n**, **4p**−**4s**, **4u**, and **4v** including $^1H$ and $^{13}C$ NMR spectra (Figures S7−S40) (PDF)

Molecular formula strings (CSV)

## ■ AUTHOR INFORMATION


### Corresponding Authors

**Thomas J. J. Müller** − *Institute of Organic Chemistry and Macromolecular Chemistry, Heinrich Heine University Düsseldorf, D-40225 Düsseldorf, Germany*; Phone: +49 211 8112298; Email: ThomasJJ.Mueller@hhu.de

**Rainer Kalscheuer** − *Institute of Pharmaceutical Biology and Biotechnology, Heinrich Heine University Düsseldorf, 40225 Düsseldorf, Germany*; orcid.org/0000-0002-3378-2067; Phone: +49 211 8114180; Email: rainer.kalscheuer@hhu.de

### Authors

**Nidja Rehberg** − *Institute of Pharmaceutical Biology and Biotechnology, Heinrich Heine University Düsseldorf, 40225 Düsseldorf, Germany*

**Gereon A. Sommer** − *Institute of Organic Chemistry and Macromolecular Chemistry, Heinrich Heine University Düsseldorf, D-40225 Düsseldorf, Germany*

**Daniel Drießen** − *Institute of Organic Chemistry and Macromolecular Chemistry, Heinrich Heine University Düsseldorf, D-40225 Düsseldorf, Germany*

**Marco Kruppa** − *Institute of Organic Chemistry and Macromolecular Chemistry, Heinrich Heine University Düsseldorf, D-40225 Düsseldorf, Germany*

**Emmanuel T. Adeniyi** − *Institute of Pharmaceutical Biology and Biotechnology, Heinrich Heine University Düsseldorf, 40225 Düsseldorf, Germany*




https://dx.doi.org/10.1021/acs.jmedchem.0c00826
J. Med. Chem. XXXX, XXX, XXX−XXX

**Shang Chen** − *Beijing Advanced Innovation Center for Food Nutrition and Human Health, College of Veterinary Medicine, China Agricultural University, Beijing 100193, China;* orcid.org/0000-0002-4874-2922
**Lin Wang** − *Institute of Pharmaceutical Biology and Biotechnology, Heinrich Heine University Düsseldorf, 40225 Düsseldorf, Germany*
**Karina Wolf** − *Institute of Pharmaceutical Biology and Biotechnology, Heinrich Heine University Düsseldorf, 40225 Düsseldorf, Germany*
**Boris O. A. Tasch** − *Institute of Organic Chemistry and Macromolecular Chemistry, Heinrich Heine University Düsseldorf, D-40225 Düsseldorf, Germany*
**Thomas R. Ioerger** − *Department of Computer Science, Texas A&M University, College Station, Texas 77843, United States*
**Kui Zhu** − *Beijing Advanced Innovation Center for Food Nutrition and Human Health, College of Veterinary Medicine, China Agricultural University, Beijing 100193, China;* orcid.org/0000-0001-8242-3952

Complete contact information is available at: https://pubs.acs.org/10.1021/acs.jmedchem.0c00826

### Author Contributions

[⊥]N.R., G.A.S., D.D., M.K., and E.T.A. contributed equally.

### Author Contributions

G.A.S. synthesized compounds **1a**, **4a**−**4f**, **4n**, and **4r**−**4s**. B.O.A.T. synthesized compounds **1a**, **4g**−**4i**, **4k**, **4o**, and **4t**. D.D. optimized the protocol for the pseudo three-component synthesis of heteroaryl bridged bisindoles and synthesized compounds **4j**, **4n**, **4p**, and **4q**. M.K. synthesized compounds **4l**, **4m**, **4u**, and **4v** and determined the solubility and stability of compounds. N.R. and E.T.A. conducted experiments involving MRSA and other bacteria. L.W. performed cell culture cytotoxicity profiling. E.T.A. measured hemolytic activity. K.W. purified pyruvate kinase and characterized the *in vitro* activity. S.C. and K.Z. performed mouse experiments. T.R.I. analyzed the whole genome sequencing data. R.K., T.J.J.M., and K.Z. designed experiments and analyzed data. N.R., G.A.S., D.D., E.T.A., T.J.J.M., and R.K. wrote the manuscript with contributions and edits from all authors.

### Notes

The authors declare no competing financial interest.

## ■ ACKNOWLEDGMENTS

G.A.S., D.D., M.K., E.T.A., R.K., and T.J.J.M. acknowledge support from the Deutsche Forschungsgemeinschaft (DFG, German Research Foundation) − project number 270650915/GRK2158. We thank Anthony R. Richardson for providing the strain *S. aureus* LAC Δ*pyk*::Erm$^{R}$. Computational support of the Zentrum für Informations- und Medientechnologie, especially the HPC team (High Performance Computing) at the Heinrich Heine University Düsseldorf, is acknowledged.

## ■ ABBREVIATIONS

MIC, minimal inhibitory concentration; MRSA, methicillin-resistant *Staphylococcus aureus*; MSSA, methicillin-sensitive *Staphylococcus aureus*; VISA, vancomycin intermediate-resistant *Staphylococcus aureus*; CFU, colony forming units; GFP, green fluorescent protein; OD, optical density; PK, pyruvate kinase; SAR, structure−activity relationship; Ni-NTA, nickel-nitrilo-acetic acid; MHB, Mueller Hinton broth; FBS, fetal bovine serum; RBC, red blood cell; COL, colistin; PI, propidium iodide; DAPI, 4′,6-diamidino-2-phenylindole

## ■ REFERENCES

(1) O'Neill, J. *Review on antimicrobial resistance: tackling a crisis for the health and wealth of nations*; https://amr-review.org/sites/default/files/SECURING%20NEW%20DRUGS%20FOR%20FUTURE%20GENERATIONS%20FINAL%20WEB_0.pdf **2015** (accessed Sept 23, 2020).
(2) WHO, W. H. O. *Global action plan on antimicrobial resistance*; http://www.who.int/antimicrobial-resistance/global-action-plan/en **2015** (accessed Sept 23, 2020).
(3) Lowy, F. D. Staphylococcus aureus infections. *N. Engl. J. Med.* **1998**, *339*, 520−532.
(4) Turner, N. A.; Sharma-Kuinkel, B. K.; Maskarinec, S. A.; Eichenberger, E. M.; Shah, P. P.; Carugati, M.; Holland, T. L.; Fowler, V. G., Jr. Methicillin-resistant Staphylococcus aureus: an overview of basic and clinical research. *Nat. Rev. Microbiol.* **2019**, *17*, 203−218.
(5) Newman, D. J.; Cragg, G. M. Natural products as sources of new drugs over the nearly four decades from 01/1981 to 09/2019. *J. Nat. Prod.* **2020**, *83*, 770−803.
(6) Haefner, B. Drugs from the deep: marine natural products as drug candidates. *Drug Discovery Today* **2003**, *8*, 536−544.
(7) Wright, A. E.; Killday, K. B.; Chakrabarti, D.; Guzmán, E. A.; Harmody, D.; McCarthy, P. J.; Pitts, T.; Pomponi, S. A.; Reed, J. K.; Roberts, B. F.; Rodrigues Felix, C.; Rohde, K. H. Dragmacidin G, a bioactive bis-indole alkaloid from a deep-water sponge of the genus Spongosorites. *Mar. Drugs* **2017**, *15*, 16.
(8) Davies-Coleman, M. T.; Veale, C. G. Recent advances in drug discovery from South African marine invertebrates. *Mar. Drugs* **2015**, *13*, 6366−6383.
(9) Netz, N.; Opatz, T. Marine indole alkaloids. *Mar Drugs* **2015**, *13*, 4814−4914.
(10) Oh, K. B.; Mar, W.; Kim, S.; Kim, J. Y.; Lee, T. H.; Kim, J. G.; Shin, D.; Sim, C. J.; Shin, J. Antimicrobial activity and cytotoxicity of bis(indole) alkaloids from the sponge Spongosorites sp. *Biol. Pharm. Bull.* **2006**, *29*, 570−573.
(11) Lim, H. K.; Bae, W.; Lee, H. S.; Jung, J. Anticancer activity of marine sponge Hyrtios sp. extract in human colorectal carcinoma RKO cells with different p53 status. *Biomed. Res. Int.* **2014**, *2014*, 413575.
(12) Tsuda, M.; Takahashi, Y.; Fromont, J.; Mikami, Y.; Kobayashi, J.'i. Dendridine A, a bis-indole alkaloid from a marine sponge Dictyodendrilla Species. *J. Nat. Prod.* **2005**, *68*, 1277−1278.
(13) Bharate, S. B.; Manda, S.; Mupparapu, N.; Battini, N.; Vishwakarma, R. A. Chemistry and biology of fascaplysin, a potent marine-derived CDK-4 inhibitor. *Mini Rev. Med. Chem.* **2012**, *12*, 650−664.
(14) Wright, A. E.; Pomponi, S. A.; Cross, S. S.; Mccarthy, P. A new bis(indole) alkaloid from a deep-water marine sponge of the genus Spongosorites. *J. Org. Chem.* **1992**, *57*, 4772−4775.
(15) Zhu, L. H.; Chen, C.; Wang, H.; Ye, W. C.; Zhou, G. X. Indole alkaloids from Alocasia macrorrhiza. *Chem. Pharm. Bull (Tokyo)* **2012**, *60*, 670−673.
(16) Endo, T.; Tsuda, M.; Fromont, J.; Kobayashi, J.'i. Hyrtinadine A, a bis-indole alkaloid from a marine sponge. *J. Nat. Prod.* **2007**, *70*, 423−424.
(17) Suzuki, A. Cross-coupling reactions of organoboranes: an easy way to construct C-C bonds (Nobel Lecture). *Angew. Chem. Int. Ed. Engl.* **2011**, *50*, 6722−6737.
(18) Hajduk, P. J.; Bures, M.; Praestgaard, J.; Fesik, S. W. Privileged molecules for protein binding identified from NMR-based screening. *J. Med. Chem.* **2000**, *43*, 3443−3447.
(19) Drießen, D.; Stuhldreier, F.; Frank, A.; Stark, H.; Wesselborg, S.; Stork, B.; Müller, T. J. J. Novel meriolin derivatives as rapid apoptosis inducers. *Bioorg. Med. Chem.* **2019**, *27*, 3463−3468.
(20) Murata, M.; Oyama, T.; Watanabe, S.; Masuda, Y. Palladium-catalyzed borylation of aryl halides or triflates with dialkoxyborane: A

novel and facile synthetic route to arylboronates. *J Org Chem* **2000**, *65*, 164−168.
(21) Broutin, P.-E.; Čerňa, I.; Campaniello, M.; Leroux, F.; Colobert, F. Palladium-catalyzed borylation of phenyl bromides and application in one-pot Suzuki-Miyaura biphenyl synthesis. *Org. Lett.* **2004**, *6*, 4419−4422.
(22) Baudoin, O.; Cesario, M.; Guénard, D.; Guéritte, F. Application of the palladium-catalyzed borylation/Suzuki coupling (BSC) reaction to the synthesis of biologically active biaryl lactams. *J. Org. Chem.* **2002**, *67*, 1199−1207.
(23) Merkul, E.; Schäfer, E.; Müller, T. J. J. Rapid synthesis of bis(hetero)aryls by one-pot Masuda borylation-Suzuki coupling sequence and its application to concise total syntheses of meridianins A and G. *Org. Biomol. Chem.* **2011**, *9*, 3139−3141.
(24) Tasch, B. O. A.; Bensch, L.; Antovic, D.; Müller, T. J. J. Masuda borylation-Suzuki coupling (MBSC) sequence of vinylhalides and its application in a one-pot synthesis of 3,4-biarylpyrazoles. *Org. Biomol. Chem.* **2013**, *11*, 6113−6118.
(25) Tasch, B. O. A.; Merkul, E.; Müller, T. J. J. One-pot synthesis of diazine-bridged bisindoles and concise synthesis of the marine alkaloid hyrtinadine A. *Eur. J. Org. Chem.* **2011**, *2011*, 4532−4535.
(26) Witulski, B.; Buschmann, N.; Bergsträßer, U. Hydroboration and Suzuki-Miyaura coupling reactions with the electronically modulated variant of an ynamine: The synthesis of (E)-β-arylenamides. *Tetrahedron* **2000**, *56*, 8473−8480.
(27) Wiese, A.; Gutsmann, T.; Seydel, U. Towards antibacterial strategies: studies on the mechanisms of interaction between antibacterial peptides and model membranes. *J. Endotoxin Res.* **2003**, *9*, 67−84.
(28) Liu, Y.; Ding, S.; Dietrich, R.; Märtlbauer, E.; Zhu, K. A Biosurfactant-Inspired Heptapeptide with Improved Specificity to Kill MRSA. *Angew. Chem. Int. Ed. Engl.* **2017**, *56*, 1486−1490.
(29) Zoraghi, R.; Worrall, L.; See, R. H.; Strangman, W.; Popplewell, W. L.; Gong, H.; Samaai, T.; Swayze, R. D.; Kaur, S.; Vuckovic, M.; Finlay, B. B.; Brunham, R. C.; McMaster, W. R.; Davies-Coleman, M. T.; Strynadka, N. C.; Andersen, R. J.; Reiner, N. E. Methicillin-resistant Staphylococcus aureus (MRSA) pyruvate kinase as a target for bis-indole alkaloids with antibacterial activities. *J. Biol. Chem.* **2011**, *286*, 44716−44725.
(30) Zoraghi, R.; Campbell, S.; Kim, C.; Dullaghan, E. M.; Blair, L. M.; Gillard, R. M.; Reiner, N. E.; Sperry, J. Discovery of a 1,2-bis(3-indolyl)ethane that selectively inhibits the pyruvate kinase of methicillin-resistant Staphylococcus aureus over human isoforms. *Bioorg. Med. Chem. Lett.* **2014**, *24*, 5059−5062.
(31) El-Sayed, M. T.; Zoraghi, R.; Reiner, N.; Suzen, S.; Ohlsen, K.; Lalk, M.; Altanlar, N.; Hilgeroth, A. Novel inhibitors of the methicillin-resistant Staphylococcus aureus (MRSA)-pyruvate kinase. *J. Enzyme Inhib. Med. Chem.* **2016**, *31*, 1666−1671.
(32) Labrière, C.; Gong, H.; Finlay, B. B.; Reiner, N. E.; Young, R. N. Further investigation of inhibitors of MRSA pyruvate kinase: Towards the conception of novel antimicrobial agents. *Eur. J. Med. Chem.* **2017**, *125*, 1−13.
(33) Zoraghi, R.; See, R. H.; Gong, H.; Lian, T.; Swayze, R.; Finlay, B. B.; Brunham, R. C.; McMaster, W. R.; Reiner, N. E. Functional analysis, overexpression, and kinetic characterization of pyruvate kinase from methicillin-resistant Staphylococcus aureus. *Biochemistry* **2010**, *49*, 7733−7747.
(34) Kumar, N. S.; Dullaghan, E. M.; Finlay, B. B.; Gong, H.; Reiner, N. E.; Selvam, J. J. P.; Thorson, L. M.; Campbell, S.; Vitko, N.; Richardson, A. R.; Zoraghi, R.; Young, R. N. Discovery and optimization of a new class of pyruvate kinase inhibitors as potential therapeutics for the treatment of methicillin-resistant Staphylococcus aureus infections. *Bioorg. Med. Chem.* **2014**, *22*, 1708−1725.
(35) Koh, J.-J.; Zou, H.; Lin, S.; Lin, H.; Soh, R. T.; Lim, F. H.; Koh, W. L.; Li, J.; Lakshminarayanan, R.; Verma, C.; Tan, D. T. H.; Cao, D.; Beuerman, R. W.; Liu, S. Nonpeptidic amphiphilic xanthone derivatives: Structure−activity relationship and membrane-targeting properties. *J. Med. Chem.* **2016**, *59*, 171−193.
(36) Hu, Y.; Amin, M. N.; Padhee, S.; Wang, R. E.; Qiao, Q.; Bai, G.; Li, Y.; Mathew, A.; Cao, C.; Cai, J. Lipidated peptidomimetics with improved antimicrobial activity. *ACS Med. Chem. Lett.* **2012**, *3*, 683−686.
(37) Gonzalez-Delgado, L. S.; Walters-Morgan, H.; Salamaga, B.; Robertson, A. J.; Hounslow, A. M.; Jagielska, E.; Sabała, I.; Williamson, M. P.; Lovering, A. L.; Mesnage, S. Two-site recognition of Staphylococcus aureus peptidoglycan by lysostaphin SH3b. *Nat. Chem. Biol.* **2020**, *16*, 24−30.
(38) Smelt, J. P. P. M.; Rijke, A. G. F.; Hayhurst, A. Possible mechanism of high pressure inactivation of microorganisms. *High Pressure Res.* **1994**, *12*, 199−203.
(39) Johnston, M. D.; Hanlon, G. W.; Denyer, S. P.; Lambert, R. J. W. Membrane damage to bacteria caused by single and combined biocides. *J Appl Microbiol* **2003**, *94*, 1015−1023.
(40) Rehberg, N.; Akone, H. S.; Ioerger, T. R.; Erlenkamp, G.; Daletos, G.; Gohlke, H.; Proksch, P.; Kalscheuer, R. Chlorflavonin targets acetohydroxyacid synthase catalytic subunit IlvB1 for synergistic killing of Mycobacterium tuberculosis. *ACS Infect Dis.* **2018**, *4*, 123−134.
(41) Costanza, F.; Padhee, S.; Wu, H.; Wang, Y.; Revenis, J.; Cao, C.; Li, Q.; Cai, J. Investigation of antimicrobial PEG-poly(amino acid)s. *RSC Adv.* **2014**, *4*, 2089−2095.
(42) Meier, D.; Hernández, M. V.; van Geelen, L.; Muharini, R.; Proksch, P.; Bandow, J. E.; Kalscheuer, R. The plant-derived chalcone xanthoangelol targets the membrane of Gram-positive bacteria. *Bioorg. Med. Chem.* **2019**, *27*, 115151.


https://dx.doi.org/10.1021/acs.jmedchem.0c00826
J. Med. Chem. XXXX, XXX, XXX−XXX